Submitted to *Operations Research*
manuscript (Please, provide the manuscript number!)

A Bayesian Real Options Model for Adaptation to Catastrophic Risk under Climate Change Uncertainty

Chi Truong
Faculty of Business and Economics, Macquarie University, NSW, Australia, 2109, chi.truong@mq.edu.au

Stefan Trück
Faculty of Business and Economics, Macquarie University, NSW, Australia, 2109, stefan.trueck@mq.edu.au

Tak Kuen Siu
Faculty of Business and Economics, Macquarie University, NSW, Australia, 2109, Ken.Siu@mq.edu.au

Michael Goldstein
Babson College, goldstein@babson.edu

We present a novel framework for the valuation of investments to mitigate risks from extreme climate events. Our model allows for decision-making on investments, taking into account deep uncertainty about climate change, and how this uncertainty changes when future climate observations become available. We show that the model is useful even when the time required to resolve uncertainty is indefinite. We further examine the impact of risk and uncertainty on optimal decisions, also comparing our results to a situation where the net present value (NPV) rule is used to guide investment. In an empirical application, we implement the model for bushfire risk management in a region in New South Wales, Australia. Our findings suggest that adaptation decisions based on the NPV rule are typically not optimal and result in a significant loss, since the value of the investment option is ignored. Further results from conducted sensitivity analysis suggest that the loss is large when the investment cost is high, when the uncertainty resolution is slow, or when the probability belief in climate change is low. Importantly, the proposed framework is also consistent with the precautionary principle, leading to earlier investment under high uncertainty together with a low rate of learning.

Key words: Climate Change Adaptation; Decision-Making under Uncertainty; Real Options Analysis; Catastrophic Risk; Bayesian Models

History: This paper was first submitted on May 23, 2019.

1. Introduction

This paper uses recently developed tools in real options theory and actuarial studies to examine investment decision-making for adaptation to extreme climate events. Different from previous studies that focus on the notion of risk, we consider also the impact of deep uncertainty that characterises situations in which different data-generating mechanisms for the climate system are regarded by the decision maker as plausible. In our framework, the decision maker learns more about the impacts of climatic change over time and uses the Bayes' rule to update her belief. Investment decisions are then made based on the information available at the current time, but with the expectation that new information will become available in the future. We investigate the impact of risk and uncertainty on the optimal investment decision, and the possible losses that incur when the net present value (NPV) rule is used to guide investment.

Significant developments in real options theory over the last two decades have made real options a popular method for the valuation of irreversible investments. In stochastic environments, where project values are uncertain and investment is irreversible, the rational decision to invest is analogous to the optimal exercise of an American option. Thus, an investment option can be easily valued and the option should be relinquished only when the value of the project is sufficiently high above the investment cost. Real options theory has been used to explain firms' investment behaviour that cannot be explained by the discounted cash flow theory (Quigg 1993, Carey and Zilberman 2002) and has been applied in various fields of research, see, e.g., Dixit and Pindyck (1994), Cortazar et al. (1998), Kenyon and Tompaidis (2001), Kogut and Kulatilaka (2001), Lambrecht and Perraudin (2003), Schwartz and Trigeorgis (2004), Marcus and Anderson (2006), Koussis et al. (2013), Hellmann and Thijssen (2018) for an overview.

Despite the appeal of real options theory in guiding investment under uncertainty, few applications exist in the area of climate change adaptation, especially in the valuation of projects that may mitigate catastrophic risks. This seems surprising, since investment projects in this area, e.g. flood dykes or dams, often last for decades and investment is therefore difficult, if not impossible, to reverse. The demand for accurate valuation of such adaptation projects is certainly high, given the enormous investment costs. In addition, uncertainty induced by climate change is immense and the most significant impact of climate change is often thought to be through rare but catastrophic events (Weitzman 2009, Jongman et al. 2014). As a result, the importance of 'real options thinking' in the field of climate change has been recognised by, e.g., Gollier and Treich (2003), Truong and Trück (2016), Truong et al. (2018).

The main difficulty in applying existing real options models to climate change adaptation is that typically in these models, the underlying probability law describing investment payoffs is assumed to be known (Dixit and Pindyck 1994). Therefore, in most of the standard real options models, only the investment payoff is uncertain and varies stochastically over time. While this assumption is reasonable in a stationary environment, it may not be suitable in the context of climate change adaptation, where the climate system is known to be changing[1], but the extent of the change is uncertain. Appropriate models need to take into account not only uncertainty about parameters in stochastic models, which is usually called 'deep uncertainty', but also how the uncertainty resolves over time as more observations on climate change impacts become available. In the absence of a scientifically rigorous model, climate change adaptation studies often revert to discounted cashflow theory and use the NPV rule to make investment decisions (West et al. 2001, Waters et al. 2003, Brouwer and van Ek 2004, Zhu et al. 2007, Kirshen et al. 2008, Bouwer et al. 2010, Mathew et al. 2012).

In this paper, we examine an optimal investment problem at a regional level to reduce the risk of climate-impacted hazards such as bushfires, flooding and storm surges. These are important

[1] As shown in Hartmann et al. (2014), observed data on global mean temperature indicates an increase of 0.075°C per decade if a linear model is estimated for the period 1901-2012, and 0.107°C per decade if a piece-wise linear model is used. For Australia, data over the period 1957-1996 indicates that occurrences of warm temperature extreme events have increased, while the number of extremely cool temperature events has decreased (Collins et al. 2000).

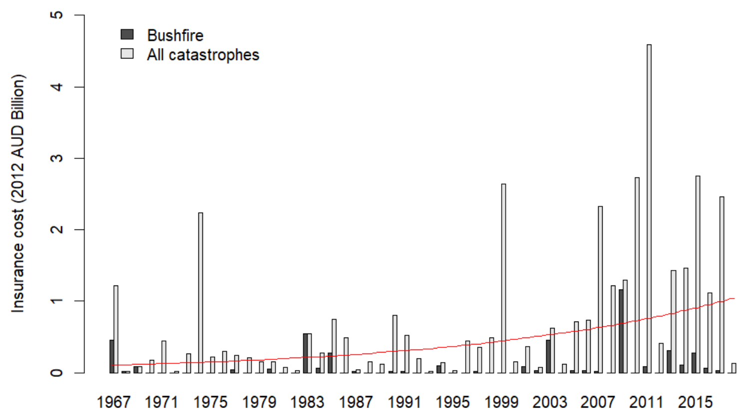

Figure 1 Inflation-adjusted annual insurance claim payments for bushfires, and all catastrophes in Australia over the period 1990-2012. The red line represents the constant growth model fitted to losses from all catastrophes. Data are sourced from Insurance Council of Australia (2016).

catastrophes that result in large costs to the insurance industry worldwide. In a warmer and therefore more energetic climate system, these catastrophes are predicted to occur even more frequently in future periods (Solomon 2007). While climatic change can be expected to increase the risk of extreme weather events globally, in our empirical analysis we focus on the application of the developed framework to a region in Australia. Recent studies suggest that Australia will be particularly impacted by climatic change with a predicted increase in the occurrence of floods, storm surges, and bushfires (Murphy and Timbal 2008, Garnaut 2011). As illustrated by Figure 1, these trends seem to be already present in the records of Australian insurance costs (Insurance Council of Australia 2016). The costs of insuring bushfire, flooding and storm surge losses appear to have grown exponentially over the last two decades, from a total of \$0.47 billion in the 1990s to \$5.2 billion in the 2000s. This expansion is likely to have been driven not just by the increase in the frequency and strength of climate-related catastrophic events, but also by changes in the underlying socio-economic environment, e.g. increased income per capita, higher cost of infrastructure, greater perception of risk (Mohleji and Pielke Jr 2014).

As a result of more frequent and possibly more severe catastrophic losses, the payoff of risk reduction investment projects is expected to grow over time. The growth rate of the payoffs is, however, highly uncertain, due to the uncertainty in climate change predictions and in the mechanisms used to downscale global climate change estimates to a regional level. Using alternative climate models and emission scenarios leads to quite different predictions for the frequency and severity of climate impacted hazards. Importantly, a decision maker can form an initial probability belief on the growth of investment payoff based on the predictions from climate models and update this belief when more observations on the impact of local climate, and therefore catastrophic risk, are available.

We contribute to the literature by introducing a real options framework for the valuation of catastrophic risk mitigation projects that allows for continuous Bayesian updating of information. Our framework is built upon work in the field of investment under incomplete information (Décamps et al. 2005, Klein 2009) but quite significantly extends these studies in several directions. First, we allow for a more general payoff structure: while Décamps et al. (2005) and Klein (2009) examine so-called 'front-loaded' projects, i.e. projects where all payoffs are obtained immediately upon investment, we investigate the investment decision for a 'back-loaded' project, where payoffs are spread across the entire lifetime of the project which is assumed to be indefinite. This extension is important since in the real world, most investment projects for catastrophe prevention or adaptation to climate change last for a long time, and payoffs are typically obtained while the projects are still in place. The investment behaviour for back-loaded projects can also be significantly different from that for front-loaded projects. We find that the optimal investment boundary in the payoff-belief state space for a back-loaded project is non-increasing rather than non-decreasing in belief as found by Décamps et al. (2005) and Klein (2009) for front-loaded projects. This means that the more pessimistic the decision maker is about the growth rate of the payoff flow, the longer she delays investment. Second, our framework allows for also growth in loss exposure that applies to most of economic regions due to economic and population growth. Third, we extend the framework to allow for risk aversion behaviour using the Esscher transform theory that is popular in the insurance literature. Fourth, we provide an empirical framework to demonstrate the application of the proposed model using available data while the studies by Décamps et al. (2005) and Klein (2009) are purely theoretical.

Our study is also related to earlier work on climate change policy that examines the impact of model uncertainty, e.g. Kelly and Kolstad (1999), Baker (2006), Karp and Zhang (2006), Berger et al. (2017). Although Bayesian studies in climate change policy such as Karp and Zhang (2006) also deal with deep uncertainty, their simulation optimization approach is time consuming and requires a prohibitively large amount of computational effort. In addition, there is no guarantee that the simulation algorithm converges (Hu et al. 2012). In contrast, we use a method of measure change that simplifies the problem considerably and makes it possible to derive some theoretical insights. When the logarithm of the investment payoff follows a random walk process without drift, we can obtain the exact value of the investment option using a closed form solution. When this is not the case, the model can be solved using standard numerical techniques such as, e.g. binomial lattice or finite difference methods. We show that when the growth rate of catastrophes' frequency is uncertain, the value of the investment option is higher than the value obtained when the growth rate is known. The decision maker would therefore prefer to have the investment option under uncertain growth rate and also want to delay investment further to learn more about the true growth rate. Investment delay is however reduced by the growth of loss exposure, the seriousness of climate change, and the strength of climate change belief. We also find that when climate change is believed to be more likely than the business usual scenario, higher uncertainty about climate change can result in shorter delay in investment, a result that is similar to the results obtained by Berger et al. (2017) under the uncertainty aversion framework.

We also analyse the expected time to learn about the growth rate of payoffs from the investment and the expected time to investment that are of great interest in climate change adaptation (Chao and Hobbs 1997, Kelly and Kolstad 1999). In contrast to the usual perception, see, e.g. Grenadier and Malenko (2010), in a modelling framework with an unknown growth rate, uncertainty may remain unresolved forever and one may never know the true growth rate. We show that the expected time to investment may also be infinite, but it is still important to use the real options framework to capture the positive value generated by volatile investment payoffs. In our case study, we find that it may take hundreds of years for climate change uncertainty to resolve, and it is therefore paramount to have a framework that can guide investment while the uncertainty remains.

The remainder of the paper is organized as follows. Section 2 outlines and analyzes the developed modeling framework. Section 3 provides an application of the framework in a case study, using catastrophic risks from bushfires as an empirical example. The final Section 4 concludes and provides some suggestions for future research in related areas.

2. Modeling framework

2.1. Frequency and Severity of Climate Impacted Hazards

We model the cumulative loss S_t over a period $(0,t]$ as a compound Poisson process:

$$S_t = \sum_{n=1}^{N_t} e^{\gamma \tau_n} X_n, \tag{1}$$

where N_t is the number of catastrophic events occurring during period $(0,t]$, γ is the growth rate of loss exposure, τ_n is the random time when the n^{th} climate impacted event occurs, and X_n is the loss caused by the n^{th} event under zero growth loss exposure. It is assumed that X_n, $n = 1, 2, \cdots$, are independent and identically distributed random variables, which are also independent of N_t. The expected value of X_n is denoted by β. We assume that the number of catastrophic events, N_t, follows a conditional Poisson process that has a stochastic intensity Λ_t, and the process $\{\Lambda_t\}$ follows a geometric Brownian motion:

$$d\Lambda_t/\Lambda_t = \mu dt + \sigma dB_t, \tag{2}$$

where $\{B_t\}$ is a standard Brownian motion defined on a given complete probability space $(\Omega, \mathcal{F}, P)$. We assume that the volatility σ is a known constant, while the drift μ is a random variable on $(\Omega, \mathcal{F}, P)$, taking a value in the state space $\{\mu_H, \mu_L\}$[2].

[2] In general, one may consider the situation where μ can take any real values. In particular, if μ has a prior distribution as a normal distribution, we may end up with a conjugate-prior situation and the posterior estimate of μ can be

The decision maker has an initial belief p_0 that the growth rate is μ_H and updates her belief as information about the Poisson intensity emerges, using the Bayes' rule, so that the information updating is rational. The σ-field generated by the process $\{\Lambda_t\}$ up to and including time t augmented by all P-null subsets of $\mathcal{F}$ is denoted by $\mathscr{F}_t$ and the posterior probability of event $\mu = \mu_H$ at time t is denoted by P_t, i.e. $P_t = P[\mu = \mu_H | \mathscr{F}_t]$, with the initial condition $P_0 = p_0$. Upon applying Bayes' rule, the posterior probability P_t can be expressed as

$$P_t = \left[1 + \frac{1-p_0}{p_0}\left(\exp\left(\ln\Lambda_t - \ln\Lambda_0 - \frac{\mu_H + \mu_L - \sigma^2}{2}t\right)\right)^{-\omega/\sigma}\right]^{-1}, \tag{3}$$

where $\omega = \frac{\mu_H - \mu_L}{\sigma}$ is interpreted as the signal to noise ratio. It can be checked that $P_t \in (0,1)$.

Note that in updating belief, we use a transformed variable $\ln\Lambda_t$ that is normally distributed and easy to work with statistically. Variable transformation, however, also changes the expected value of the variable via the Jensen inequality effect when the transformation is non-linear. For a known growth rate μ, the expected value of Λ_t is $\Lambda_0 e^{\mu t}$ while the expected value of $\ln\Lambda_t$ is not $\ln\Lambda_0 + \mu t$, but a lower value $\ln\Lambda_0 + \mu t - \sigma^2 t/2$.

It is apparent from Equation (3) that in updating belief, we compare the value of $\ln\Lambda_t$ with the reference point $\ln\Lambda_0 + \frac{\mu_H + \mu_L - \sigma^2}{2}t$, which is the midpoint of the expected values of $\ln\Lambda_t$[3]. If $\ln\Lambda_t$ is higher than the reference point, belief P_0 is revised upwards and vice versa. The extent of revision is proportional to the difference between $\ln\Lambda_t$ and the reference point, the level of uncertainty $\mu_H - \mu_L$, and is inversely proportional to the noise level measured by σ.

We can describe the dynamics of the posterior belief P_t by using another Brownian motion $\{\bar{B}_t\}$ that is adapted to the filtration $\{\mathscr{F}_t\}$[4],

$$\bar{B}_t \equiv \sigma^{-1}\left(\ln\Lambda_t - \ln\Lambda_0 - \int_0^t E(\mu|\mathscr{F}_s)ds + \frac{1}{2}\sigma^2 t\right). \tag{4}$$

derived by solving a heat equation, as in, for example, Karatzas and Zhao (2001) and Zhang et al. (2012). However, to illustrate the key idea of the present modeling framework and to simplify our discussion, we consider the simpler situation where μ takes a value in $\{\mu_H, \mu_L\}$

[3] Note that the expected value under the low growth rate is $\ln\Lambda_0 + \mu_L t - \sigma^2 t/2$, and under the high growth rate is $\ln\Lambda_0 + \mu_H t - \sigma^2 t/2$.

[4] Note that the Brownian motion $\{B_t\}$ is not adapted to the filtration $\{\mathscr{F}_t, t \geq 0\}$, since μ is unknown and therefore, knowing the history of Λ_t up to time t is not sufficient to know the history of B up to time t.

As discussed in Liptser and Shiryaev (2001), Chapter 7, Section 7.4, the (observed) dynamics of Λ_t can then be expressed in terms of $\bar{B}_t$ as

$$d\Lambda_t/\Lambda_t = [\mu_L + P_t(\mu_H - \mu_L)]dt + \sigma d\bar{B}_t, \tag{5}$$

and by applying Itô's Lemma to (3), the dynamics of posterior beliefs can be obtained,

$$dP_t = P_t(1 - P_t)\frac{(\mu_H - \mu_L)}{\sigma}d\bar{B}_t. \tag{6}$$

A posterior belief satisfying (6) has a zero expected rate of change and at any point in time, the current belief is the best forecast of future belief. Indeed $\{P_t\}$ is an $(\mathbb{F}, P)$-(local)-martingale. Due to the fact that $P_t \in (0,1)$, it is an $(\mathbb{F}, P)$-martingale. In addition, the variation in the posterior belief is proportional to the signal to noise ratio. When the noise (σ) is large, posterior beliefs change slowly since new observations convey little information about the growth rate μ. When the difference between high and low growth rates, $\mu_H - \mu_L$, is large and the noise is small, new observations may reveal the true value of μ and the posterior belief experiences a large change.

2.2. Investments into Climate Change Adaptation

Let us now consider an investment project with investment cost I that is sunk once committed. The project reduces the frequency of catastrophic events by a proportion k from the investment time until infinity. Since the expected loss over a period $(t_1, t_2]$, given the information observed up to and including time t_1, is $\beta E[\int_{t_1}^{t_2} e^{\gamma s}\Lambda_s ds|\mathscr{F}_{t_1}]$, the investment payoff over this period is $k\beta E[\int_{t_1}^{t_2} e^{\gamma s}\Lambda_s ds|\mathscr{F}_{t_1}]$. Let $\pi_t = k\beta e^{\gamma t}\Lambda_t$ be the benefit flow of the project at time t. Since Λ_t follows process (5), π_t evolves according to process:

$$d\pi_t/\pi_t = [\gamma + \mu_L + P_t(\mu_H - \mu_L)]dt + \sigma d\bar{B}_t. \tag{7}$$

At the discount rate r, the expected NPV of investing in the project at time τ, conditional on the information available up to and including time $t \geq 0$, is given by

$$E\left[\int_{\tau}^{\infty} e^{-r(s-t)}\pi_s ds - e^{-r(\tau-t)}I|\mathscr{F}_t\right]. \tag{8}$$

The decision maker determines an optimal time to enter into the investment project that maximizes the expected NPV. Admission investment times are non-anticipative (i.e., depend only on the current information, but not on future information), which is the case if τ is a stopping time. Thus, the optimal investment problem can be formulated as:

$$\max_{\tau \in \Gamma_{t,\infty}} E\left[\int_{\tau}^{\infty} e^{-r(s-t)}\pi_s ds - e^{-r(\tau-t)} I | \mathscr{F}_t\right], \tag{9}$$

where $\mathscr{F}_t$ represents the information available up to and including time t, and $\Gamma_{t,\infty}$ is the space of all $\mathbb{F}$-stopping times, taking a value in the interval $[t,\infty)$, and $\{\pi_t\}$ evolves according to processes (6) and (7).

This problem has two state variables, P_t and π_t that are correlated. It may not be easy to directly calculate the NPV of a project invested at a given state, while determining the value of the option is even more challenging. In the following, we therefore apply a change of measures method to simplify the problem.

2.3. A Measure Change Approach

The investment problem may now be simplified by changing the measure P to $\tilde{P}$ under which π_s has a known and constant growth rate of $\gamma + \mu_L$. This measure change approach has been used in filtering and is called a reference probability approach, see, for example, Elliott et al. (1995). The measure change is achieved by using the Radon-Nikodym derivative Z_∞ such that

$$\left.\frac{d\widetilde{P}}{dP}\right|_{\mathcal{F}_\infty} := Z_\infty, \tag{10}$$

where $Z_s = \exp\left(-\int_t^s \theta_u d\bar{B}_u - \frac{1}{2}\int_t^s \theta_u^2 du\right)$, and $\theta_s = P_s\omega$. Since $P_s \in (0,1)$, $|\theta_s|$ is bounded, and as a result, $\{Z_s\}$ is an $(\mathbb{F}, P)$-martingale. Indeed, it is an uniformly integrable martingale, and so $\lim_{s\to\infty} Z_s = Z_\infty$, P-a.s. Under $\tilde{P}$, $\tilde{B}_s = \bar{B}_s + \int_t^s \theta_u du$ is a standard Brownian motion by Girsanov's theorem, (see, for example, Karatzas and Shreve (1988), Chapter 3, Section 3.5). To simplify the problem, we replace the state variable P_s by the likelihood ratio $\phi_s = \frac{P_s}{1-P_s}$ that evolves over time according to the stochastic differential equation $d\phi_s = \omega\phi_s d\tilde{B}_s$. By a version of the Bayes' rule, the investment problem then becomes

$$F(\phi_t,\pi_t) = \max_{\tau} \tilde{E}\left[\frac{1}{Z_\infty}\left(\int_\tau^\infty e^{-r(s-t)}\pi_s ds - e^{-r(\tau-t)}I\right)|(\phi_t,\pi_t)\right] \tag{11}$$

subject to the dynamic state constraints

$$d\pi_s/\pi_s = (\gamma+\mu_L)ds + \sigma d\tilde{B}_s, \tag{12}$$

$$d\phi_s/\phi_s = \omega d\tilde{B}_s, \quad s \geq t. \tag{13}$$

Note that in (11), $Y_s \equiv Z_s^{-1}$ is a martingale under measure $\tilde{P}$ that has an initial starting point $Y_t = 1$, and the value at time s can be expressed in terms of ϕ_s as $Y_s = \frac{1+\phi_s}{1+\phi_t}$[5]. Using the value $Z_s^{-1} \equiv Y_s = \frac{1+\phi_s}{1+\phi_t}$ and Lemma 1, we can express (11) as

$$F(\phi_t,\pi_t) = \frac{1}{1+\phi_t}\max_{\tau}\tilde{E}\left[\left(\int_\tau^\infty e^{-r(s-t)}(1+\phi_s)\pi_s ds - e^{-r(\tau-t)}(1+\phi_\tau)I\right)|(\phi_t,\pi_t)\right]. \tag{14}$$

Lemma 1. *Let*

$$H = \tilde{E}\left[\frac{1}{Z_\infty}\left(\int_\tau^\infty e^{-r(s-t)}\pi_s ds\right)|(\phi_t,\pi_t)\right], \tag{15}$$

where Z_∞ is given by (10) and π_t follows process (12). Then, H can also be expressed as:

$$H = \tilde{E}\left[\left(\int_\tau^\infty e^{-r(s-t)}\frac{1}{Z_s}\pi_s ds\right)|(\phi_t,\pi_t)\right]. \tag{16}$$

See EC.6 for proof.

2.4. Risk Aversion by the Esscher Transform

In this section, we present the method to incorporate risk aversion into our modelling framework. Specifically, we use the Esscher transform that provides a convenient way to incorporate risk aversion via changing probability measures. In this approach, the Esscher parameter can be interpreted

[5] As shown in EC.6, Y_s evolves according to the stochastic differential equation $dY_s/Y_s = \theta_s d\tilde{B}_s$. In addition, since $\theta = P\omega = \frac{\phi}{1+\phi}\omega$ and $d\phi_s = \phi_s\omega d\tilde{B}_s$, we have $dY_s/Y_s = d\phi_s/(1+\phi_s)$. Therefore, two variables Y_s and $X_s \equiv \frac{1+\phi_s}{1+\phi_t}$ follows the same stochastic process and both have the same initial value of 1. As a result, $Y_s = \frac{1+\phi_s}{1+\phi_t}$.

as the risk premium required to compensate for risk aversion in the decision making process. In practice, the Esscher parameter might be extracted through different methods such as experiments, estimation from empirical data in climate sciences, or from premiums charged for related insurance contracts.

Let $\{\eta(s)\}$ be the process of the Esscher parameters. It is supposed that $\{\eta(s)\}$ is predictable with respect to the observed filtration $\{\mathcal{F}(s)\}$. Loosely speaking, for each s, $\eta(s)$ is known given the observed information $\mathcal{F}(s-)$ up to just prior to time s. Then the density process for changing probability measures under the Esscher transform associated with the process $\{\eta(s)\}$ is given by:

$$Z^{\eta}(s) = \exp\left(\int_t^s \eta(u)\sigma d\tilde{B}(u) - \frac{1}{2}\int_t^s \eta^2(u)\sigma^2 du\right), \tag{17}$$

It can be shown that $\{Z^{\eta}(s)\}$ is an $\{\mathcal{F}(s)\}$-martingale. See EC.1 for the technical details about the Esscher transform.

A new probability measure P^{η} equivalent to $\tilde{P}$ on $\mathcal{F}_{\infty}$ can now be defined by putting:

$$\left.\frac{dP^{\eta}}{d\tilde{P}}\right|_{\mathcal{F}_{\infty}} := Z^{\eta}(\infty). \tag{18}$$

It is known by the Girsanov's theorem for Brownian motions that under the new measure P^{η}, the process $\{B^{\eta}(t)\}$ defined by

$$B^{\eta}(s) := \tilde{B}(s) - \int_t^s \eta(u) du,$$

is a standard Brownian motion with respect to the observed filtration $\{\mathcal{F}(s)\}$. Consequently, under P^{η}, the stochastic benefit flow $\{\pi(s)\}$ is governed by the following dynamics:

$$d\pi(s)/\pi(s) = (\gamma + \mu_L + \sigma\eta(s))ds + \sigma dB^{\eta}(s), \tag{19}$$

and similarly, $\phi(s)$ evolves according to the stochastic process:

$$d\phi(s)/\phi(s) = \eta(s)\omega ds + \omega dB^{\eta}(s). \tag{20}$$

It is apparent that risk aversion increases the drift of the benefit flow $\{\pi_s\}$ and renders the benefit to grow faster. For a given level of risk aversion, a higher volatility σ will result in a higher drift for the process $\{\pi_s\}$. Similarly, risk aversion increases the likelihood ratio, and strengthens the belief in the more serious climate change scenario.

Equations (19-20) can be solved to obtain a time dependent relation between ϕ_s and π_s:

$$\frac{\phi_s}{\phi_t} = \left(\frac{\pi_s}{\pi_t}\right)^{\omega/\sigma} \exp\left[-\frac{\omega(s-t)}{2\sigma}(2\gamma + \mu_H + \mu_L - \sigma^2)\right]. \tag{21}$$

From here, we can see that the Esscher parameter representing the risk premium attributed to risk aversion is incorporated in the drift of the stochastic intensity process under the new measure P^η selected by the Esscher transform. To incorporate the risk premium in the valuation of the investment option, in the next sub-section, we shall work with the new probability measure P^η. For the sake of generality, the theoretical framework presented here incorporates time-varying, or stochastic risk premiums, which are given by the process $\{\eta(s)\}$ of the Esscher parameters. However, for the numerical implementation later on, we assume, for simplicity, that the risk premium is a constant and its value can be determined by an estimate, using e.g. insurance data, to characterize risk aversion.

2.5. Valuation of the Investment Option

The actuarial value of the option to invest at state (ϕ_t, π_t) under the new measure P^η defined in the last sub-section is:

$$F(\phi_t, \pi_t) = \frac{1}{1+\phi_t} \max_{\tau} E^\eta \left[\left(\int_\tau^\infty e^{-r(s-t)}(1+\phi_s)\pi_s ds - e^{-r(\tau-t)}(1+\phi_\tau)I\right) |(\phi_t, \pi_t)\right], \tag{22}$$

where E^η is the expectation under the measure P^η, and under the new measure P^η, the dynamics of the state processes are given by (19) and (20).

To find the value of the investment option, we solve the auxiliary optimal stopping problem:

$$G(\phi_t, \pi_t) = \max_{\tau\in\Gamma_{t,\infty}} E^\eta \left[\left(\int_\tau^\infty e^{-r(s-t)}(1+\phi_s)\pi_s ds - e^{-r(\tau-t)}(1+\phi_\tau)I\right) |(\phi_t, \pi_t)\right]. \tag{23}$$

LEMMA 2. *In the optimal stopping problem (23), the intrinsic value obtained by immediate stopping at time t is:*

$$V(\phi_t,\pi_t)=\frac{\pi_t}{r-\gamma-\mu_L-\eta\sigma}+\frac{\pi_t\phi_t}{r-\gamma-\mu_H-\eta(\sigma+\omega)}-(1+\phi_t)I. \tag{24}$$

see EC.2 for proof.

At any time t, given state (ϕ_t,π_t), the decision to be made is whether to stop and get value $V(\phi_t,\pi_t)$ or to wait to the next instant $t+\Delta t$. The value $G(\phi_t,\pi_t)$ is the larger of the value obtained by immediate stopping and the value obtained by waiting,

$$G(\phi_t,\pi_t)=\max\{V(\phi_t,\pi_t),e^{-r\Delta t}E^{\eta}\left[G(\phi_{t+\Delta t},\pi_{t+\Delta t})|(\phi_t,\pi_t)\right]\}. \tag{25}$$

Suppose that the value function G is "sufficiently" smooth in the continuation region, i.e. $G\in\mathcal{C}^2$, where $\mathcal{C}^2$ is the space of twice continuously differentiable functions. Using Itô's lemma and standard arguments in optimal stopping theory[6], we can express (25) as:

$$\begin{aligned}&\max\big(V(\phi_t,\pi_t)-G(\phi_t,\pi_t),\\&\quad\frac{1}{2}\sigma^2\pi_t^2G_{\pi\pi}+\frac{1}{2}\omega^2\phi_t^2G_{\phi\phi}-\omega\sigma\phi_t\pi_tG_{\phi\pi}-\omega\eta_t\phi_tG_{\phi}+(\gamma+\mu_L+\eta_t\sigma)\pi_tG_{\pi}-rG\big)=0,\end{aligned} \tag{26}$$

where the subscripts of G denote the derivatives of function G. In the continuation region (i.e., deferring investment), the value of the option can be found by solving the second-order partial differential equation:

$$\frac{1}{2}\sigma^2\pi_t^2G_{\pi\pi}+\frac{1}{2}\omega^2\phi_t^2G_{\phi\phi}-\omega\sigma\phi_t\pi_tG_{\phi\pi}-\omega\eta_t\phi_tG_{\phi}+(\gamma+\mu_L+\eta_t\sigma)\pi_tG_{\pi}-rG=0. \tag{27}$$

In addition, at the optimal investment threshold (ϕ^*,π^*), the following high-contact and smooth-pasting conditions need to be satisfied[7]:

$$G(\phi^*,\pi^*)=V(\phi^*,\pi^*) \tag{28}$$

[6] see, for example, Shiryaev (1978), Chapter 3, and Oksendal (2003), Chapter 10, Section 10.4

[7] In the context of pricing finite-maturity American-style contingent claims, some theoretical justifications for the high-contact and smooth-pasting conditions are available in the literature, see, for example, Elliott and Kopp (2005), Chapter 8, for the case of a geometric Brownian motion, and a recent paper by Siu (2016) for the case of a self-exciting threshold diffusion process.

$$G_\phi(\phi^*, \pi^*) = V_\phi(\phi^*, \pi^*) \tag{29}$$

$$G_\pi(\phi^*, \pi^*) = V_\pi(\phi^*, \pi^*). \tag{30}$$

In general cases, the partial differential equation (27) may not have a closed form solution. The option value can be found by applying finite difference methods to (27) or a lattice method to (25). Note that for a lattice method, starting from an initial state (ϕ_t, π_t), the value of ϕ_s can be determined based on π_s, and the lattice has one state variable. This is much simpler than solving (27) with two state variables. We therefore use a binomial lattice method to calculate the option value and the optimal investment threshold (see EC.7 for details on binomial lattice method). We also assume that $\eta_s = \eta$, which is a given constant.

2.6. Special Case

As shown in (21), when $\gamma + \frac{\mu_H + \mu_L}{2} = \frac{1}{2}\sigma^2$, the two state variables of the investment problem map one to one in a time homogeneous relation. Consider ϕ_t as a parameter, the problem then has only one state variable π_t. The optimal stopping time is the first time when π_t exceeds the optimal threshold π^* that is a function of parameter ϕ_t.

The condition of the special case is imposed on the sum of γ, μ_H and μ_L, and therefore, for a given σ, there are various combinations of γ, μ_H and μ_L for which the special case applies. This makes the special case relevant to most of the empirical contexts.

2.6.1. The Investment Threshold

PROPOSITION 1. *If $\gamma + \frac{\mu_H + \mu_L}{2} = \frac{1}{2}\sigma^2$, the optimal stopping time that solves Problem (23) is a trigger strategy with $\tau^* = \inf\{s : \pi_s \geq \pi^*\}$. The investment threshold π^* depends on the belief at the time of investing P^* and is defined by:*

$$\pi^* = \frac{P^*\alpha_H + (1 - P^*)\alpha_L}{P^*(\alpha_H - 1)V_H + (1 - P^*)(\alpha_L - 1)V_L} \times I, \tag{31}$$

where $\alpha_L = \frac{1}{2} - (\gamma + \mu_L + \sigma\eta)/\sigma^2 + \sqrt{((\gamma + \mu_L + \sigma\eta)/\sigma^2 - \frac{1}{2})^2 + 2r/\sigma^2}$ is the solution of the quadratic equation:

$$\frac{1}{2}\sigma^2\alpha_L(\alpha_L - 1) + (\gamma + \mu_L + \sigma\eta)\alpha_L - r = 0. \tag{32}$$

In addition, $\alpha_H = \alpha_L - \omega/\sigma$, $V_H = \frac{1}{r-\gamma-\mu_H-\eta(\sigma+\omega)}$ *and* $V_L = \frac{1}{r-\gamma-\mu_L-\eta\sigma}$.

See EC.3 for proof.

Equation (31) suggests that the optimal investment threshold π^* is a function of belief at investment, P_t. As shown in Proposition 2, the optimal investment threshold is decreasing in belief, in contrast to the results by Décamps et al. (2005) and Klein (2009) who find that the optimal investment threshold is increasing in belief. The optimal investment threshold π^* is also found to be decreasing in belief in the general case, as illustrated in Figure 7 in the empirical section.

In the case examined by Décamps et al. (2005) and Klein (2009), the value of the project is assumed to be observed directly, and increases in the current belief affect only future values of the project, leaving the current value of the project unaffected. An increase in the current belief will increase the expected growth rate of the project value, and reduce the shortfall between the risk free rate and the expected growth rate of the project value[8]. The investment threshold is therefore increased, and project investment is deferred further into the future. In our case, the value of the project is the total present value of all future payoffs, and therefore, an increase in the current belief will also increase the current value of the project. As long as an increase in the current belief generates a higher impact on the current project value compared to the impact on the investment boundary (when investment boundary is defined in terms of project value), increases in the current belief will result in earlier investment.

Proposition 2. *Suppose* $\gamma + \frac{\mu_H+\mu_L}{2} = \frac{1}{2}\sigma^2$ *and* $\eta = 0$, *then* $d\Lambda^*/dP^* < 0$. *See EC.4 for proof.*

Note that our investment threhold in (31) takes a generalised form of the investment threshold of a standard real options model. In the standard real options, the investment threshold satisfies $V^* = \frac{\alpha}{\alpha-1}I$ or $V^*\frac{(\alpha-1)}{\alpha} = I$, see, e.g. Dixit and Pindyck (1994). In the case of uncertain growth rate, the ratio of belief weighted average of $(\alpha-1)V$ to the belief weighted average of α is equal to the investment cost at the investment threshold, i.e. $\frac{E[(\alpha-1)V]}{E(\alpha)} = I$, where E is the expectation under distribution $(P_t, (1-P_t))$ of the growth rate (μ_H, μ_L).

[8] As discussed in Truong et al. (2018), the shortfall is similar to the dividend payout rate, and when the shortfall is zero, the project will never be invested. A higher shortfall will result in earlier investment.

2.6.2. Option Value

PROPOSITION 3. *When $\gamma + \frac{\mu_H + \mu_L}{2} = \frac{1}{2}\sigma^2$, the value of the investment option at state (P_t, π_t) is:*

$$F(P_t,\pi_t) = P_t\left(\frac{\pi_t}{\pi^*}\right)^{\alpha_H}\left(\frac{\pi^*}{r-\gamma-\mu_H-\eta(\sigma+\omega)} - I\right) + (1-P_t)\left(\frac{\pi_t}{\pi^*}\right)^{\alpha_L}\left(\frac{\pi^*}{r-\gamma-\mu_L-\eta\sigma} - I\right) \tag{33}$$

See EC.3 for proof.

Thus, the option value is a belief-weighted average of the corresponding values obtained in certainty cases. When $P_t = 0$ or $P_t = 1$, Equations (31) and (33) provide the investment threshold and the option value for the case when the growth rate is known with certainty to be μ_L or μ_H, which are consistent with the standard real options model outlined in Dixit and Pindyck (1994).

2.7. Impacts of Volatility

In the proposed model, the volatility parameter σ also represents the noise that makes the distinction between the high growth rate μ_H and the low growth rate μ_L difficult. One may expect that an increase in σ will reduce the value of waiting, and the value of the option to invest.

However, as shown in Proposition 4, increases in volatility actually lead to increases in the investment threshold. This seems quite obvious from the value of the option given in (33), where the option value of investment is the weighted average of an option value under the high growth rate μ_H and an option value under the low growth rate μ_L. It is well-known that the option value under a given growth rate (μ_H or μ_L) is increasing in σ. As a result, an increase in σ will increase the option value under μ_H and the option value under μ_L, and therefore increase the option value of the investment. In addition, since the investment threshold is increasing for both μ_H and μ_L, the investment threshold given by the Bayesian real options model will increase when volatility σ increases. The impact of volatility is further illustrated in Figure 2.

PROPOSITION 4. *For $\gamma + \frac{\mu_H + \mu_L}{2} = \frac{1}{2}\sigma^2$ and $\eta = 0$, the optimal investment threshold π^* is increasing in volatility σ. See EC.9 for proof.*

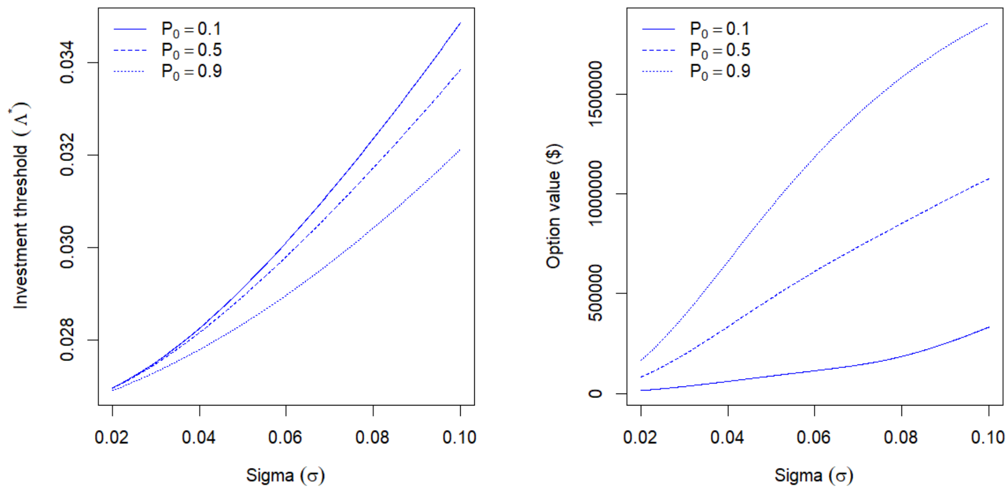

Figure 2 Impacts of volatility σ on the investment threshold and the option value for different initial belief P_0.

2.7.1. Impacts of Uncertainty In the proposed model, uncertainty is represented by the difference in possible drifts, $\mu_H - \mu_L$. To enable comparison with the results by Klein (2009), we examine the special case where $\gamma + \frac{\mu_H + \mu_L}{2} = \frac{1}{2}\sigma^2$ and $\eta = 0$. In this case, an increase in uncertainty means a mean preserving spread of the drifts.

Figure 3 illustrates the impact of uncertainty on the investment threshold and the option value for different initial beliefs. To facilitate benchmarking, we also depict the case where the drift is known and equal to the expected drift, $P_0\mu_H + (1 - P_0)\mu_L$[9]. When the initial belief is $P_0 = 0.5$, increases in uncertainty do not change the expected value $P_0\mu_H + (1 - P_0)\mu_L$, and the impact of uncertainty becomes most apparent. As shown in Proposition 5, uncertainty and the opportunity to learn about the true drift, in fact, increase the value of the investment option and make it worthwhile to wait longer than when the drift is known with certainty. It is clear that a decision maker would prefer the case of uncertainty, where the option to invest has a higher value.

[9] In this case, the investment threshold is $\hat{\pi} = \frac{\hat{\alpha}}{(\hat{\alpha}-1)} I(r - \gamma - \hat{\mu})$ where $\hat{\mu} = P_0\mu_H + (1 - P_0)\mu_L$, and $\hat{\alpha} = \frac{1}{2} - (\gamma + \hat{\mu})/\sigma^2 + \sqrt{[(\gamma + \hat{\mu})/\sigma^2 - \frac{1}{2}]^2 + 2r/\sigma^2}$. The option value is $\hat{F}(\pi_t) = B\pi_t^{\hat{\alpha}}$, where $B = \left(\frac{1}{r-\gamma-\hat{\mu}} \frac{\hat{\alpha}-1}{\hat{\alpha}}\right)^{\hat{\alpha}} \frac{I^{1-\hat{\alpha}}}{\hat{\alpha}-1}$, see Truong et al. (2018) for details.

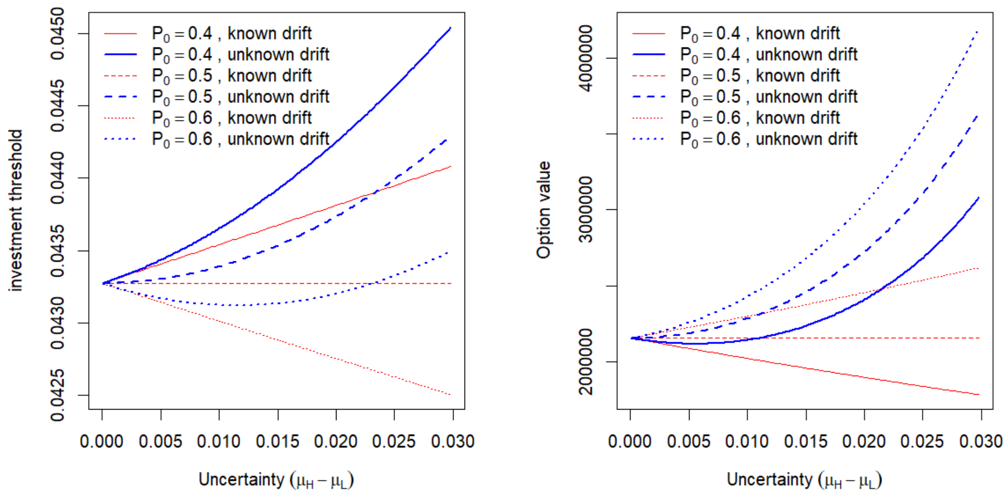

Figure 3 Impacts of drift uncertainty on the investment threshold and the option value for different initial belief P_0. Thin lines represent the cases where the standard real options model is used with the drift assumed known and equal to $P_0\mu_H + (1-P_0)\mu_L$.

PROPOSITION 5. *For $\gamma + \frac{\mu_H+\mu_L}{2} = \frac{1}{2}\sigma^2$ and $\eta = 0$, the optimal investment threshold $\pi^*(P_0)$ under drift uncertainty is higher than the investment threshold $\hat{\pi}(P_0)$ for the case when the drift is known and equal to $\hat{\mu} = P_0\mu_H + (1-P_0)\mu_L$. See EC.8 for proof.*

The finding that the investment threshold is higher in the uncertainty case, as stated in Proposition 5, is different from the results found by Klein (2009) for front-loaded projects where projects with uncertain drift are invested earlier. This difference suggests that it is important to explicitly model backloaded projects when investment payoffs are harvested over the lifetime of the projects.

Although relative to the case of drift certainty, investment delay is increased under drift uncertainty, the relation between uncertainty and investment timing is in general non-monotonic. As shown in Figure 3, when the initial belief is higher than 0.5, increases in uncertainty will increase the expected drift $\hat{\mu}$ and reduces the investment threshold under the known drift $\hat{\mu}$. The optimal investment threshold under uncertain drift also decreases as long as the uncertainty is not excessively large. The result that uncertainty can increase or decrease the option value and the investment threshold is consistent with the findings by Klein (2009), and broadly consistent with Miao and Wang (2011) who find that uncertainty ambiguity can accelerate or delay option exercise.

2.8. Learning Time

The expected time required to learn about the true growth rate with a level of confidence, e.g. 95% confidence, provides an indication of how slowly or quickly the uncertainty is resolved. We are $X\%$ confident that the true growth rate is μ_H when the belief P_t reaches $X\%$. Conversely, we are $X\%$ confident that the true growth rate is μ_L when P_t reaches $(100-X)\%$.

We can find the expected time to learn about μ_H when the true growth rate is μ_H as follows. When the true growth rate is μ_H, the value of Λ_t at time t is given by:

$$\Lambda_t = \Lambda_0 \exp\left[(\mu_H - \frac{\sigma^2}{2})t + \sigma B_t\right]. \tag{34}$$

Using (34) in Equation (3) gives:

$$\frac{\mu_H - \mu_L}{2} t + \sigma B_t = \frac{\sigma}{\omega} \ln\left[\frac{P_t}{1-P_t} \frac{1-p_0}{p_0}\right]. \tag{35}$$

Therefore, we will be $X\%$ confident that the true growth rate is μ_H when the process $Y_t = \frac{\mu_H-\mu_L}{2}t + \sigma B_t$ reaches a value $\frac{\sigma}{\omega}\ln\frac{X}{100-X}\frac{1-p_0}{p_0}$. Apply the results of Lemma 3 with $x=0$, $a=\frac{\mu_H-\mu_L}{2}$ and $m=\frac{\sigma}{\omega}\ln\frac{X}{100-X}\frac{1-p_0}{p_0}$, the expected time to learn about the true growth rate μ_H is:

$$E(\tau_H) = \frac{2}{\omega^2} \ln\left[\frac{X}{100-X}\frac{1-p_0}{p_0}\right]. \tag{36}$$

This implies that the expected time to learn about the true growth rate μ_H is lower when the signal to noise ratio is higher or when the initial belief p_0 is higher. Similarly, the expected time to learn about the true growth rate μ_L is

$$E(\tau_L) = \frac{2}{\omega^2} \ln\left[\frac{X}{100-X}\frac{p_0}{1-p_0}\right]. \tag{37}$$

such that the expected time to learn about the true growth rate μ_L is lower when the signal to noise ratio is higher or when the initial belief p_0 is lower.

Lemma 3. *Consider a process $dX_t = adt + \sigma dB_t$, where B_t is a Brownian motion, $X_0 = x > 0$, and a stopping time $\tau_m = \min\{t \geq 0 : X_t = m\}$. Then*

$$E\tau_m = \begin{cases} \frac{m-x}{a} & \text{if } \frac{m-x}{a} \geq 0 \\ \infty & \text{otherwise.} \end{cases} \tag{38}$$

For proof, see EC.5

2.8.1. Expected Investment Delay The expected time to investment can be calculated as

$$E\tau_{\pi^*} = p_0 E[\tau_{\pi^*}|\mu = \mu_H] + (1 - p_0) E[\tau_{\pi^*}|\mu = \mu_L]. \quad (39)$$

The expected time $E[\tau_{\pi^*}|\mu = \mu_i], i \in \{H, L\}$ is the time for process $d\ln\pi_t = (\gamma + \mu_i - \frac{1}{2}\sigma^2)dt + \sigma dB_t$ to get to the optimal investment threshold π^* from π_0. Apply Lemma 3:

$$E[\tau_{\pi^*}|\mu = \mu_i] = (\gamma + \mu_i - \frac{1}{2}\sigma^2)^{-1} \ln \frac{\pi^*}{\pi_0}, \quad i \in \{H, L\}.$$

Note that when $\gamma + \mu_L - \frac{1}{2}\sigma^2 < 0$, $E[\tau_{\pi^*}|\mu = \mu_L]$ is infinite and as a result, the expected time to investment $E\tau_{\pi^*}$ is infinite. An important question is whether the real options framework is still relevant. This question can be answered by looking at the case $p_0 = 0$, i.e. the growth rate is known with certainty to be μ_L, and the investment problem is reduced to the standard real options problem considered in the literature. If the volatility is positive, there is a positive probability that the value of the project will rise above the current level in the future and deferring investment to a later time may provide a higher value. As it is well-known from the real options literature, see, e.g. Dixit and Pindyck (1994), (and also apparent from (31)), when $\sigma > 0$, the investment threshold in terms of project value is $\frac{\alpha_L}{\alpha_L - 1} I$, which is higher than I. This holds regardless of the expected time to investment. The investment threshold given by our real options model is, therefore, optimal even when the expected investment delay or the expected time taken for uncertainty to resolve is infinite.

3. Empirical Application

We illustrate the application of the proposed model by examining a case study of bushfire risk management in Ku-ring-gai local government area in NSW, Australia. The area has residential properties in close proximity to bushland and ranks third in bushfire vulnerability among the 61 local government areas in the Greater Sydney Region.

A number of options has been identified by Ku-ring-gai Council to reduce the risk from bushfires. These include, among others, building new fire trails, constructing new fire stations and rezoning land, see Ku-ring-gai Council (2010). Fire trails allow for controlled hazard reduction burning, break wild fire transition and potentially allow more time for fire brigades to respond to bushfires. Constructing more fire stations reduces the response time and helps to reduce the risk of fires expanding beyond suppression. In the following, we will focus on evaluating an adaptation project of constructing an additional fire trail in the region.[10]

3.1. Bushfire Risk Estimation

Implementation of the investment model requires an estimate of parameters μ and σ of the expected fire frequency process Λ_t. To estimate the volatility σ, we use daily data of the McArthur Forest Fire Danger Index (FFDI) that is commonly used to provide fire warnings in Australia and also other countries. The McArthur Forest Fire Danger Index combines air temperature, wind speed, humidity and a drought factor to forecast the chance that a bush fire will occur on a specific day in a local area.[11] It has also been used in previous studies to examine the changes in bush fire risk under climate change, see e.g. Jolly et al. (2015), Clarke et al. (2016).

Figure 4 shows the monthly FFDI in Sydney, which is obtained by aggregating daily FFDI observations for each month. It is apparent that the FFDI contains seasonal variation and exhibits additional volatility due to the variation in local weather conditions. For the investment decision, we are mainly interested in the long term variation of the FFDI that results from changes in climatic conditions. We therefore use a dynamic factor model to extract a common factor that drives the long term variation of the FFDI in various regions in Australia. Our approach is similar to the approach proposed by Schwartz and Smith (2000) to extract the long term component from a commodity price process. The difference is that Schwartz and Smith (2000) use futures price data with different maturities, while in our case, such data are not available, and as an alternative, we use observations for the FFDI in different locations in Australia.

[10] Note that Truong et al. (2018) examine sequential investment projects, but considering a single project only allows us to better illustrate our framework.

[11] Note that in NSW, Australia, the Forest Fire Danger Index is reported on a scale from 0-100, but should not be interpreted as actual probability for the occurrence of a bushfire, see, e.g., Lucas (2010) for further details.

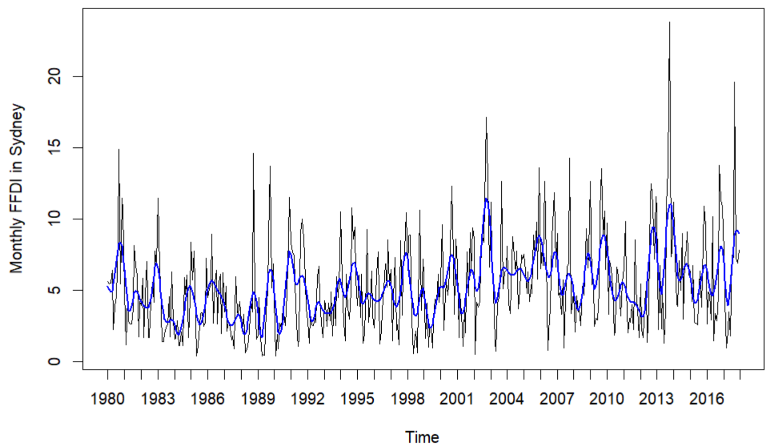

Figure 4 Monthly cumulative FFDI for the Sydney region in NSW.

We model the logarithm of the total FFDI in month t and region i as:

$$\log \mathrm{FFDI}_{i,t} = b_{1,i} f_t + b_{2,i} s_t + \epsilon_{i,t}, \tag{40}$$

where $b_{1,i}$ and $b_{2,i}$ are the factor loadings to be estimated and $\epsilon_{i,t} \sim N(0, \sigma^2_{\epsilon_i})$. The common trend f_t is assumed to follow a random walk with drift, and the seasonality factor s_t follows a deterministic periodic pattern:

$$f_t = f_{t-1} + \delta_{t-1} + \xi_t, \quad \xi_t \sim N(0, \sigma^2_\xi) \tag{41}$$

$$\delta_t = \delta_{t-1} \tag{42}$$

$$s_t = -\sum_{j=1}^{11} s_{t-j}. \tag{43}$$

The error terms, $\epsilon_{i,t}$ and η_t, are assumed to be uncorrelated with each other and uncorrelated with their past values. The model can be written in state space form as:

$$\log \mathrm{FFDI}_{i,t} = b_i X_t + \epsilon_{i,t}, \tag{44}$$

$$X_t = T X_{t-1} + R\xi_t, \tag{45}$$

where $b_i = [\, b_{1,i} \ 0 \ b_{2,i} \ 0 \ \ldots \ 0]$, $X_t = [\, f_t \ \delta_t \ s_t \ s_{t-1} \ \ldots \ s_{t-10}]'$, $R = [\, 1 \ 0 \ 0 \ 0 \ \ldots \ 0]'$, and $T(13 \times 13)$ is a state transition matrix.

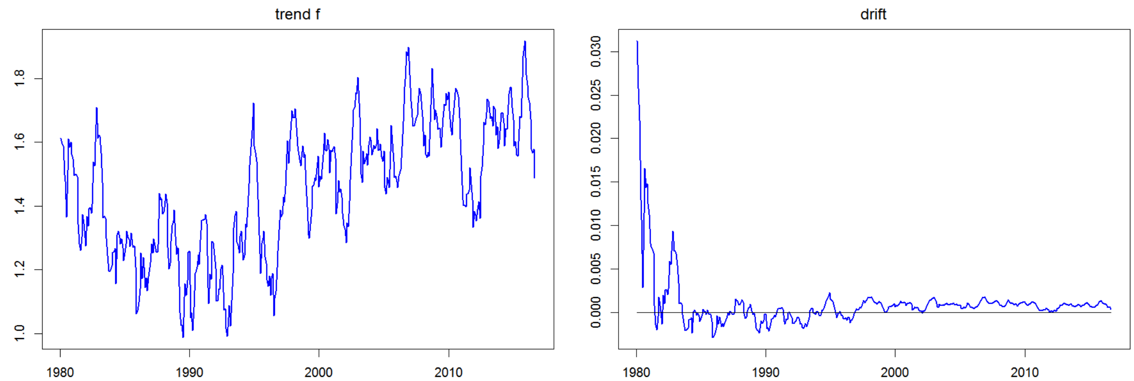

Figure 5 Estimates of long term trend (f_t) and its drift (δ_t) based on the applied dynamic factor model

We estimate this state space model using a Kalman filter as documented in e.g. Durbin and Koopman (2012). For the model to be identified, we set the factor loadings of the risk in the first region, $b_{1,1}$ and $b_{1,3}$ to be equal to 1.

To obtain reliable estimates of the long term risk processes, we use the FFDI data observed in the capital cities of four large states of Australia, i.e. Sydney, Melbourne, Perth and Hobart. These data are based on measurements from weather stations at airports and have good quality.

The estimates of the long term risk factor f_t and the drift δ_t are presented in Figure 5. The long term risk factor seems to decrease over period 1980-1990, and starts to trend up since 1990. The estimate of the drift obtained from the dynamic factor model is essentially a Bayesian estimate. In the initial periods, with short data samples, the drift estimates are more volatile, and after the year 2000 when the samples are sufficiently long, the drift estimates are consistently positive. However, significant uncertainty remains about the exact value of the drift.

3.1.1. Estimating the frequency of events We obtain the Poisson intensity for Ku-ring-gai by downscaling the deseasonalized forest fire danger index of the Sydney region in NSW. In the Ku-ring-gai area, there was only one house-damaging bushfire event occuring over period 1980-2017 (38 years), and the average probability of an event occurring in one year is $1/38 = 0.026$. We therefore scale down the deseasonalized FFDI of the Sydney region by a factor of 2400 so that the scaled-down risk has an annual average of 0.026. The Poisson intensity for the Ku-ring-gai area is then:

$$\ln \Lambda_t = -\ln 2400 + f_t + \epsilon_t, \tag{46}$$

where $f_t \sim N(f_0 + \delta \times t, \sigma_\eta^2 \times t)$, and $\epsilon_t \sim N(0, 0.6770^2)$.

Note that for the investment problem, the investment decision depends on the state variable f_t. The measurement error term ϵ_t is only relevant in that the expected value of Λ_t and the expected value of the project are increased by $e^{0.5\times\sigma_\epsilon^2}$, otherwise, it is irrelevant to the investment decision. As a result, for investment analysis, we can use an equivalent Poisson intensity variable $\hat{\Lambda}_t$ given by:

$$\ln \hat{\Lambda}_t = -\ln 2400 + 0.5 \times \sigma_\epsilon^2 + f_t. \tag{47}$$

The volatility of process $\{\hat{\Lambda}_t\}$ is σ_η, which is also the volatility σ in Equation (2) that we need to estimate. The estimate of this volatility is 5.81% per month, and $5.81\% \times \sqrt{12} = 20.13\%$ per year. The current value of the Poisson intensity is $\hat{\Lambda}_0 = 0.0279$.

For the drift parameter μ, using a single value of drift μ estimated from historical data may not be able to reflect the uncertainty about climate change. We therefore use two values of drift μ to represent different views. We use $\mu_L = 0$ to represent a climate change skeptic view that there will be no climate change, and a value $\mu_H > 0$ estimated based on climate change studies that represents the view that the climate will change. In particular, Sharples et al. (2016) suggest that the frequency of extreme bushfire events in eastern Australia will increase by 200% from 2010 to 2100, and therefore, we set $\mu_H = 2.22\%$ per year. To estimate the initial belief P_0, we use the study by Hasson et al. (2009) who use 10 general circulation models and two GHG emission scenarios, a low (B1) and a high (A2) emission scenario, to forecast the frequency of extreme fire weather events in Southeastern Australia. Since the frequency of extreme fire weather events is found to increase in 11 out of 20 cases, we set $P_0 = 0.55$.

3.1.2. Estimating the loss severity Following Truong and Trück (2016), we estimate the loss severity distribution based on the information provided by a bushfire expert in the area. We use a gamma distribution to allow for heavy tailed bushfire losses. The expert suggests that for a severe bushfire, the average number of houses being damaged is 30 and the range for the average number of damaged houses is between 15 (the lower quartile) and 50 (the upper quartile) houses. With the reconstruction cost per house of \$405,000, the loss severity distribution has a location parameter $a = 8077.55$ and a scale parameter $s = 1504.17$, see Truong and Trück (2016) for details. The expected bushfire loss in a fire event is then $\beta = \$12.15$ million. The growth rate of loss severity (γ) is estimated based on disaster insurance claim data provided by the Insurance Council Australia (ICA) and yields a growth rate of $\gamma = 1\%$.

3.2. The Discount Rate

The choice of an appropriate discount rate for long lasting projects is a highly controversial topic in the literature. Some studies, e.g. Stern (2007) and Garnaut (2011), recommend the use of low social discount rates, largely based on intergenerational equity arguments, while others such as Newell and Pizer (2003), Nordhaus (2007), Quiggin (2008) and Tol and Yohe (2009) suggest that the discount rate should be derived based on market interest rates.

We follow the latter strand of literature to determine the discount rate based on observed market interest rates. In particular, we adopt the results by Truong and Trück (2016) who estimate the stochastic interest rate model proposed by Cox et al. (1985) using long term Australian government bond data. They found that for Australian interest rates, the estimated model yields a quite low coefficient of persistence, such that the estimated certainty equivalent discount rate converges quickly to a long run level of 4.5%. For simplicity, in this study, we assume that the discount rate is constant at 4.5%.

3.3. Other Parameters

Parameters relating to the investment project, including investment cost, risk mitigation effectiveness and project life, are estimated by expert elicitation. Expert elicitation is an effective way to

Table 1 Information on estimated and assumed parameter values.

Parameters	Value	Parameters	Value
Current Poisson intensity ($\hat{\Lambda}_0$)	0.0279	Risk mitigation by project (k)	20%
High Poisson intensity growth (μ_H)	2.22%	Risk mitigation by project (k)	20%
Low Poisson intensity growth (μ_L)	0%	Lifetime of the project (M)	50 years
Volatility of the Poisson intensity process (σ)	20.13%	Investment cost per project (I_M)	\$1.5 million
Expected loss conditional on a fire event (β)	\$12.15 M	Annual maintenance cost (C)	\$50,000
Growth rate of loss severity (γ)	1%	Risk aversion parameter (η)	2.7×10^{-4}
Discount rate (r)	4.5%	Initial belief (P_0)	0.55

overcome data scarcity problems and has been used in many previous climate adaptation studies, see e.g. Baker and Solak (2011), Mathew et al. (2012). The expert specifies that the conducted project is expected to reduce the frequency of house damaging bushfire events by 20%. The investment cost I of an infinite lifetime project can be calculated based on the estimated costs I_M for a project that lasts M years given in Table 1 as:

$$I = I_M / [1 - (1 + r)^{-(M+1)}] \tag{48}$$

Thus, at a 4.5% discount rate, the present value of building a bushfire trail with cost \$1.5 million every 50 years, is \$1.68 million.

The estimate of the risk aversion parameter η is obtained by calibration. Cummins and Weiss (2009) suggest that the premium charged by the reinsurance industry for bearing catastrophic risk is comparable with the premium charged for bearing catastrophic risk by CAT bond holders. Data on CAT bond premiums in the US over the period 2001-2008 indicate that the premium is about 5% (Cummins and Weiss 2009, p525). We therefore assume that the value of the project with risk aversion is higher than the value of the project with risk neutrality by 5%. This gives $\eta = 2.7 \times 10^{-4}$.

3.4. Optimal Decision-Making

3.4.1. Baseline Case Let us first consider a base case scenario, where parameter values are as given in Table 1. For this scenario, Figure 6 provides the plot of the option value $F(\pi_0)$, where the initial belief is $P_0 = 0.55$. For this case, at the current level of benefit flow $\pi_0 = \$67,797$, the option value is \$2,090,421, and the optimal investment threshold for the initial period is $\pi^* = \$171,450$. The expected time to learn about the growth rate with 95% confidence is 451 years when the true growth rate is μ_H, and 517 years when it is μ_L. This slow resolution of climate change uncertainty is consistent with other studies in climate change, see e.g. Leach (2007). The long learning time is due to the large value of noise (20.13%) relative to the signal (2.22%), leading to a small signal to noise ratio ($\omega = 0.03$). Given the long learning time, waiting for the uncertainty to resolve completely before taking a decision on adaptation is infeasible. It is essential to make the investment decision in the presence of climate change uncertainty. Note also that since $\mu_L - \frac{1}{2}\sigma^2 < 0$, the expected time to investment is infinite. However, as explained in Section 2.8.1, our modelling framework remains valid and allows to determine the optimal investment decision when the uncertainty is partially resolved.

The investment threshold obtained from the model is substantially higher than the threshold given by the NPV rule ($\hat{\pi} = \$49,950$). If the NPV rule was used, the project would be invested immediately, and a NPV of \$1,016,602 would be obtained. An amount of \$1,073,819 i.e. 51,37% of the option value would be lost. For other levels of belief, optimal investment decisions can be made based on the investment boundary in Figure 7. For example, if $\pi_0 = \$160,000$ and $P_0 = 0.4$, the optimal decision is to wait, while if $\pi_0 = \$190,000$ and $P_0 = 0.8$, the project should be invested. When π_0 is lower than \$150,000 (higher than \$200,000), waiting (investing) is optimal regardless of belief.

3.4.2. Impact of Initial Belief To enable a comparison with the impact of other factors, we examine the impact of an increase in the initial belief P_0 by 10% from 0.55. For this higher belief, the investment threshold is slightly lower at $\pi^* = \$168,750$ and the option value at $\pi_0 = \$67,797$ is increased by 7.90% to \$2,255,489. The NPV of the project at the current benefit flow level, $\pi_0 = \$67,797$, is increased by 18.35% to \$1,203,141 and the loss due to using the NPV rule is reduced by 2.00% to \$1,052,349.

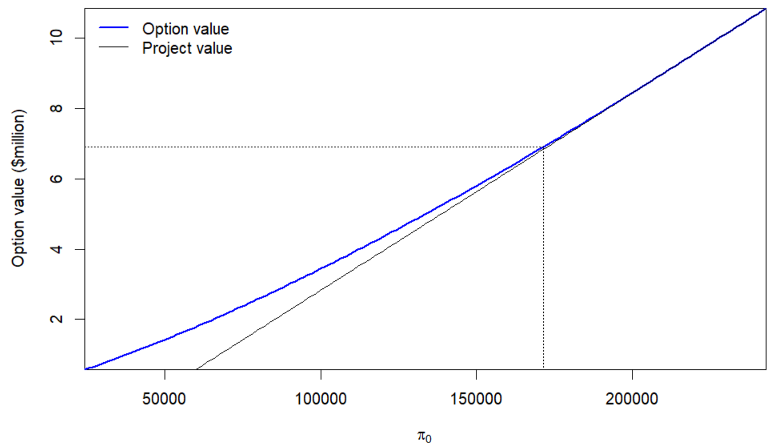

Figure 6 Investment option values, project values and investment threshold in baseline case with $P_0 = 0.5$

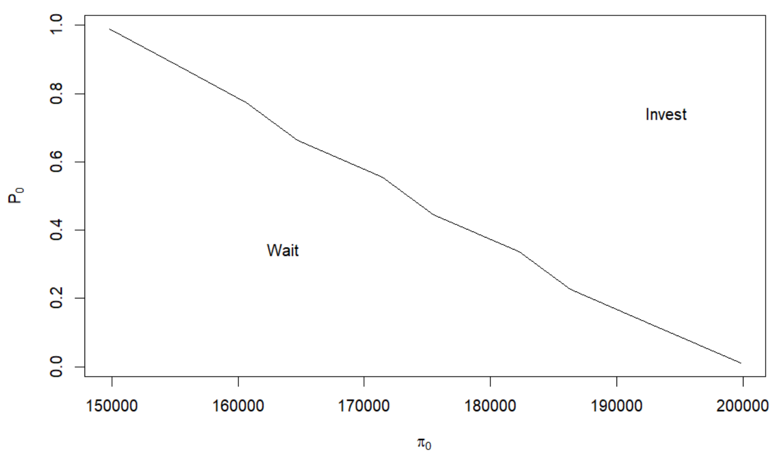

Figure 7 Investment boundary defined in two states (P_0, π_0)

3.4.3. Impact of Uncertainty The impact of uncertainty is examined by comparing the baseline scenario with the case where uncertainty is increased by 10%, i.e. μ_L is decreased to -0.1110% and μ_H is increased to 2.3310%. When the uncertainty increases by 10%, the NPV of the project at the initial state $(P_0 = 0.55, \pi_0 = \$67,797)$ increases by 25.03%. This is because the impact of risk aversion is very small (see below), and with $\eta = 0$, the NPV of the project is $V(\phi_0, \Lambda_0)/(1+\phi_0)$ is a convex function of a random variable μ that takes values $\{\mu_H, \mu_L\}$. Therefore, when the uncertainty in μ increases, the NPV of the project increases. The option value at the initial state increases by 12.13% to \$2,343,968 and the optimal investment threshold is reduced by

1.57% to \$168,750. The loss when applying a NPV rule as decision criteria is also reduced, and is 0.08% lower, i.e. \$1,072,957. These results can be interpreted as more uncertainty resulting to earlier investment, consistent with the precautionary principle.

3.4.4. Impact of Volatility When volatility increases by 10%, the NPV of the project at the initial state ($P_0 = 0.55, \pi_0 = \$67,797$) is increased, but the change is very small (0.08%). The optimal investment threshold increases by 5.51% to \$180,900 while the option value at the initial state increases by 2.74% to \$2,147,672. As a result, the loss incurred when using the NPV rule in comparison to optimal timing of the investment increases by 5.26% to \$1,130,305.

3.4.5. Impact of Risk Aversion When the risk aversion parameter η is increased by 10%, the NPV of the project is increased by 0.20% to \$1,018,679. The option value at the initial state increases by 0.09% to \$2,092,359, and the optimal investment threshold remains unchanged. The loss induced by using the NPV rule is reduced by 0.01%. Changes in the risk aversion parameter therefore do not have much impact on the investment decision.

3.4.6. Impact of Climate Change Scenarios Some climate change studies, e.g. Weitzman (2009), Keller et al. (2004), suggest that the extent of change in the future climate can be quite extreme. We examine a more serious climate change scenario in which the high level of the growth rate, μ_H, is increased by 10%. With the increase in μ_H, the NPV of the project at the initial state ($P_0 = 0.55, \pi_0 = \$67,797$) increases by 61.11% to \$1,637,852. The option value at the initial state is increased by 28.77% to \$2,691,868 and the investment threshold is reduced by 3.15% to \$166,050. Under these assumptions, the loss incurred by using the NPV rule is then reduced by 1.84% to \$1,054,016.

3.4.7. Impact of loss exposure growth rate When the growth rate of loss exposure increases by 10% from 1% to 1.10%, the NPV of the project is increased by 27.15% while the option value is increased by 12.39%. The optimal investment threshold is reduced by 2.36%, pushing investment to occur earlier. The loss due to the use of NPV rule is reduced by 1.58%.

3.4.8. Impact of Investment Costs When the investment cost increases by 10%, the NPV of the project at the initial state ($P_0 = 0.55, \pi_0 = \$67,797$) is decreased by 27.43% to $737,716. The option value at the initial state is reduced by 2.59% and the investment threshold increases by 10.23% to $189,000. The loss due to using the NPV rule in comparison to the optimal timing of the investment is then increased by20.92% to $1,298,474 . Therefore, changes in the initial investment cost may have a substantial impact on the value obtained from investing and the time when the project should be invested.

3.4.9. Impact of the Discount Rate The impact of the applied discount rate on the results is examined by comparing the baseline scenario with the case where the discount rate is increased by 10%. As a result of the higher discount rate, the NPV of the project at the initial state ($P_0 = 0.55, \pi_0 = \$67,797$) is decreased by 71.50% to $289,751. The investment threshold is increased by 4.72% to $179,550 and the option value at the initial state is significantly reduced by 34.66% to $1,365,842. The loss due to using the NPV rule therefore increases by 0.21% to $1,076,091.

3.4.10. Summary of sensitivity analysis A summary of the results for the conducted sensitivity analysis is provided in Table 2. Recall that for each variable, we examine the impact of a 10% increase in the parameter value. For our case study, we find that the loss due to using a simple NPV rule instead of optimally timing the investment increases substantially for a larger initial investment cost and a higher value of volatility. In addition, the loss is decreasing in the signal to noise ratio, i.e. the loss is higher when the uncertainty is low or when the volatility is high. This means that the real options model is more important in settings where uncertainty resolution is slow. Furthermore, the loss is decreasing in the initial belief in climate change as well as the predicted level of climate change, which is consistent with the findings of Truong and Trück (2016).

4. Conclusion

In this paper, we introduce a novel framework for determining the optimal timing of investment into catastrophic risk mitigation projects. Instead of assuming that the growth rate of catastrophe

Table 2 Sensitivity Analysis for a 10% increase in key parameters

Parameter	ΔNPV	Δ(Option value)	Δ(Investment threshold[1])	Δ(Loss by NPV rule)
Initial belief (P_0)	18.35%	7.90%	-1.57%	-2.00%
Uncertainty ($\mu_H - \mu_L$)	25.03%	12.13%	-1.57%	-0.08%
Volatility (σ)	0.08%	2.74%	5.51%	5.26%
Risk aversion (η)	0.70%	0.09%	0.00%	-0.01%
Extent of Climate Change (μ_H)	61.11%	28.77%	-3.15%	-1.84%
Loss exposure growth (γ)	27.15%	12.39%	-2.36%	-1.58%
Investment cost (I_m)	-27.43%	-2.59%	10.23%	20.92%
Discount rate (r)	-71.50%	-34.66%	4.72%	0.21%

Note: to examine the sensitivity to the initial belief, the parameter for initial belief P_0 is changed from $P_0 = 0.55$ to $P_0^* = 0.605$; to measure the sensitivity of the results to uncertainty, $\mu_H - \mu_L$ is changed from 0.0222 to 0.0244 corresponding to $\mu_L^* = -0.11\%$ and $\mu_H^* = 2.33\%$; to examine the impact of volatility, σ is increased from $\sigma = 0.2013$ to $\sigma^* = 0.2214$; to quantify the impact of a more serious climate change scenario, μ_H increases from 2.22% to 2.44%; investment costs are assumed to increase from $I_m = \$1,500,000$ to $I_m^* = \$1,650,000$; the discount rate r changes from $r = 0.045$ to $r^* = 0.0495$.

[1] The change in investment threshold is the change in the Poisson intensity, keeping belief constant.

frequency is known as it is typically proposed in real options models, our framework allows for the uncertainty about the actual growth rate. In the proposed framework, the decision maker's prior belief about the growth rate of the expected frequency of catastrophic events is combined with climate observations to inform investment decisions.

In a special case, the framework allows to derive a closed form solution for the value of the option to invest. Furthermore, the option value of investment can be expressed as a weighted average of the option values under different climate change scenarios. This means that the Bayesian real option also has the same property as the standard real option and its value increases for higher levels of volatility. There is, however, an important difference: in standard real options models, one would invest only when the NPV of the project is sufficiently higher than the investment cost to justify the volatile project value. Therefore, given a specific estimate of volatility, a higher growth rate will raise the value of the project and lower the investment threshold. At the same time, for a specific growth rate, higher volatility will raise the value of the project and also increase the investment threshold. In the Bayesian real options model, there are two levels of uncertainty: the uncertainty about the project value for a given growth rate, and the uncertainty about the true growth rate. While the impact of the volatility on the investment threshold and option value is similar to the case of a standard real option, the impact of the second layer of uncertainty is quite different. When the learning rate is low, increasing uncertainty lowers the investment threshold and accelerates investment. When the learning rate is significant, uncertainty can accelerate or decelerate investment, depending on whether the impact of learning dominates the impact of uncertainty.

The Bayesian model utilizes both prior belief and new observations to distinguish between a high and a low growth rate. In the proposed empirical application, we illustrate that it may take a relatively long time - up to several hundred years - for climate change uncertainty to resolve. An important implication of this result is that passive learning through observing the climate might play a less important role than active learning via climate change research that is represented by the prior belief in the model.

As cautioned by Mearns (2010), a slow rate of learning can be used as an argument for not acting on climate change adaptation yet. High uncertainty and a slow rate of learning might also explain why typically the NPV rule instead of a real options framework is used in climate change adaptation studies. However, based on the proposed framework we argue that the Bayesian framework provides a solution that is robust to climate change uncertainty. If the decision maker is quite uncertain about climate change, the value of the Bayesian real option is the average of the option values under different climate change scenarios. On the other hand, if the decision maker has a strong belief in a climate change scenario, the value of the Bayesian real option is strongly weighted towards the standard option value given in such scenario. Importantly, an additional feature of the framework is that the advised investment decision is consistent with the precautionary principle that has been emphasized in relation to climate change mitigation action, e.g. by the IPCC. When the climate change scenario is believed to be more likely than the business usual scenario, higher uncertainty about climatic change can result in a lower investment threshold, and the adaptation investment will occur with a shorter delay.

Our empirical results suggest that the loss due to the use of the NPV rule instead of a real options framework can be high. This is because the NPV rule ignores the option to invest, which is valuable in all climate change scenarios. We further find that the loss is larger when the noise is larger, which leads to a seemingly contradictory result that when climate change uncertainty is resolved more slowly, the loss due to the use of the NPV is higher. This is because when the noise is higher, the option value in each climate change scenario will be higher, such that the value of the Bayesian real option will also be higher. Although the increase in the noise makes it more difficult to distinguish between the scenarios, such increased difficulty in learning is irrelevant when the option to invest is ignored all together, as implied by the NPV rule. We also find that the loss is large when the investment cost is high and when the belief in climate change is low. This suggests that the proposed Bayesian real options model is most useful for large investment projects whose benefits depend on future climate and the decision maker has a low belief about the climate change scenario.

Future research could apply the proposed framework to the valuation of other investments in climate change adaptation, for example to hazards arising from flooding, storms or sea level rise. Interesting applications of the method might also include large infrastructure projects that often require information updating or resolving uncertainty about, e.g., population growth or environmental change. Also, the high sensitivity of the option value and the loss incurred by using the NPV rule to changes in volatility also provides directions for additional research. For example, there may be practical ground for the development of real options models that can also include uncertainty and learning about volatility.

References

Baker E (2006) Increasing risk and increasing informativeness: Equivalence theorems. *Operations Research* 54(1):26–36.

Baker E, Solak S (2011) Climate change and optimal energy technology R&D policy. *European Journal of Operational Research* 213(2):442–454.

Berger L, Emmerling J, Tavoni M (2017) Managing catastrophic climate risks under model uncertainty aversion. *Management Science* 63(3):749–765.

Bouwer LM, Bubeck P, Aerts JC (2010) Changes in future flood risk due to climate and development in a Dutch polder area. *Global Environmental Change* 20(3):463–471.

Boyle PP, Evnine J, Gibbs S (1989) Numerical evaluation of multivariate contingent claims. *Review of Financial Studies* 2(2):241–250.

Brouwer R, van Ek R (2004) Integrated ecological, economic and social impact assessment of alternative flood control policies in the Netherlands. *Ecological Economics* 50(1-2):1–21.

Bühlmann H, Delbaen F, Embrechts P, Shiryaev AN (1996) No-arbitrage, change of measure and conditional esscher transforms. *CWI quarterly* 9(4):291–317.

Carey JM, Zilberman D (2002) A model of investment under uncertainty: modern irrigation technology and emerging markets in water. *American Journal of Agricultural Economics* 84(1):171–183.

Chao PT, Hobbs BF (1997) Decision analysis of shoreline protection under climate change uncertainty. *Water Resources Research* 33(4):817–829.

Clarke H, Pitman AJ, Kala J, Carouge C, Haverd V, Evans JP (2016) An investigation of future fuel load and fire weather in australia. *Climatic Change* 139(3-4):591–605.

Collins D, Della-Marta P, Plummer N, Trewin B (2000) Trends in annual frequencies of extreme temperature events in Australia. *Australian Meteorological Magazine* 49(4):277–292.

Cortazar G, Schwartz ES, Salinas M (1998) Evaluating environmental investments: A real options approach. *Management Science* 44(8):1059–1070.

Cox JC, Ingersoll JE, Ross SA (1985) A theory of the term structure of interest rates. *Econometrica* 53(2):385–407.

Cox JC, Ross SA, Rubinstein M (1979) Option pricing: A simplified approach. *Journal of Financial Economics* 7(3):229–263.

Cummins JD, Weiss MA (2009) Convergence of insurance and financial markets: Hybrid and securitized risk-transfer solutions. *Journal of Risk and Insurance* 76(3):493–545.

Décamps JP, Mariotti T, Villeneuve S (2005) Investment timing under incomplete information. *Mathematics of Operations Research* 30(2):472–500.

Dixit AK, Pindyck RS (1994) *Investment under uncertainty* (Princeton, New Jersey: Princeton University Press).

Durbin J, Koopman SJ (2012) *Time series analysis by state space methods* (Oxford University Press), 2nd edition.

Elliott R, Kopp K (2005) *Mathematics of Financial Markets* (New York: Springer), 2nd edition.

Elliott RJ, Aggoun L, Moore JB (1995) *Hidden Markov models: estimation and control* (New York: Springer).

Garnaut R (2011) *The Garnaut review 2011: Australia in the global response to climate change* (Cambridge University Press).

Gerber HU, Shiu ES (1993) Option pricing by Esscher transforms (with discussion). *Transactions of the Society of Actuaries* 46:99–191.

Gollier C, Treich N (2003) Decision-making under scientific uncertainty: the economics of the precautionary principle. *Journal of Risk and Uncertainty* 27(1):77–103.

Grenadier SR, Malenko A (2010) A Bayesian approach to real options: The case of distinguishing between temporary and permanent shocks. *The Journal of Finance* 65(5):1949–1986.

Hartmann D, Tank A, Rusticucci M (2014) Observations: Atmosphere and surface. Stocker TF, ed., *Climate change 2013: the physical science basis: Working Group I contribution to the Fifth assessment report of the Intergovernmental Panel on Climate Change*, chapter 2, 159–254 (Cambridge University Press).

Hasson AEA, Mills GA, Timbal B, Walsh K (2009) Assessing the impact of climate change on extreme fire weather events over southeastern Australia. *Climate Research* 39(2):159–172.

Hellmann T, Thijssen JJJ (2018) Fear of the market or fear of the competitor? Ambiguity in a real options game. *Operations Research* 66(6):1744–1759.

Hu Z, Cao J, Hong LJ (2012) Robust simulation of global warming policies using the dice model. *Management Science* 58(12):2190–2206.

Insurance Council of Australia (2016) Historical disaster costs .

Jolly WM, Cochrane MA, Freeborn PH, Holden ZA, Brown TJ, Williamson GJ, Bowman DM (2015) Climate-induced variations in global wildfire danger from 1979 to 2013. *Nature Communications* 6:7537.

Jongman B, Hochrainer-Stigler S, Feyen L, Aerts JC, Mechler R, Botzen WW, Bouwer LM, Pflug G, Rojas R, Ward PJ (2014) Increasing stress on disaster-risk finance due to large floods. *Nature Climate Change* 4(4):264–268.

Kallsen J, Shiryaev AN (2002) The cumulant process and esscher's change of measure. *Finance and Stochastics* 6(4):397–428.

Karatzas I, Shreve S (1988) *Brownian Motion and Stochastic Calculus* (New York: Springer).

Karatzas I, Zhao X (2001) Bayesian adaptive portfolio optimization. Jouini E, Cvitanic J, Musiela M, eds., *Option Pricing, Interest Rates and Risk Management*, 632–669 (Cambridge University Press), ISBN 9780511569708.

Karp L, Zhang J (2006) Regulation with anticipated learning about environmental damages. *Journal of Environmental Economics and Management* 51(3):259–279.

Keller K, Bolker BM, Bradford DF (2004) Uncertain climate thresholds and optimal economic growth. *Journal of Environmental Economics and Management* 48(1):723–741.

Kelly DL, Kolstad CD (1999) Bayesian learning, growth, and pollution. *Journal of Economic Dynamics and Control* 23(4):491–518.

Kenyon C, Tompaidis S (2001) Real options in leasing: The effect of idle time. *Operations Research* 49(5):675–689.

Kirshen P, Knee K, Ruth M (2008) Climate change and coastal flooding in Metro Boston: impacts and adaptation strategies. *Climatic Change* 90(4):453–473.

Klein M (2009) Comment on investment timing under incomplete information. *Mathematics of Operations Research* 34(1):249–254.

Kogut B, Kulatilaka N (2001) Capabilities as real options. *Organization Science* 12(6):744–758.

Koussis N, Martzoukos SH, Trigeorgis L (2013) Multi-stage product development with exploration, value-enhancing, preemptive and innovation options. *Journal of Banking & Finance* 37(1):174–190.

Ku-ring-gai Council (2010) Climate change adaptation strategy. Technical report, Ku-ring-gai Council.

Lambrecht B, Perraudin W (2003) Real options and preemption under incomplete information. *Journal of Economic Dynamics and Control* 27(4):619–643.

Leach AJ (2007) The climate change learning curve. *Journal of Economic Dynamics and Control* 31(5):1728–1752.

Liptser R, Shiryaev AN (2001) *Statistics of Random Processes: I. General Theory* (New York: Springer).

Lucas C (2010) On developing a historical fire weather data-set for Australia. *Australian Meteorological and Oceanographic Journal* 60(1):1.

Marcus B, Anderson CK (2006) Online low-price guarantees—a real options analysis. *Operations Research* 54(6):1041–1050.

Mathew S, Trück S, Henderson-Sellers A (2012) Kochi, India case study of climate adaptation to floods: Ranking local government investment options. *Global Environmental Change* 22(1):308 – 319.

Mearns LO (2010) The drama of uncertainty. *Climatic Change* 100(1):77–85.

Miao J, Wang N (2011) Risk, uncertainty, and option exercise. *Journal of Economic Dynamics and Control* 35(4):442–461.

Mohleji S, Pielke Jr R (2014) Reconciliation of trends in global and regional economic losses from weather events: 1980–2008. *Natural Hazards Review* 15(4):04014009.

Murphy BF, Timbal B (2008) A review of recent climate variability and climate change in southeastern Australia. *International Journal of Climatology* 28(7):859–879.

Newell RG, Pizer WA (2003) Discounting the distant future: how much do uncertain rates increase valuations? *Journal of Environmental Economics and Management* 46(1):52–71.

Nordhaus WD (2007) A review of the stern review on the economics of climate change. *Journal of economic literature* 45(3):686–702.

Oksendal B (2003) *Stochastic Differential Equations: An Introduction with Applications* (New York: Springer), 6th edition.

Quigg L (1993) Empirical testing of real option-pricing models. *The Journal of Finance* 48(2):621–640.

Quiggin J (2008) Stern and his critics on discounting and climate change: an editorial essay. *Climatic Change* 89(3):195–205.

Ryan R, Lippman SA (2003) Optimal exit from a project with noisy returns. *Probability in the Engineering and Informational Sciences* 17(04):435–458.

Schwartz E, Smith JE (2000) Short-term variations and long-term dynamics in commodity prices. *Management Science* 46(7):893–911.

Schwartz ES, Trigeorgis L (2004) *Real options and investment under uncertainty: classical readings and recent contributions* (MIT press).

Sharples JJ, Cary GJ, Fox-Hughes P, Mooney S, Evans JP, Fletcher MS, Fromm M, Grierson PF, McRae R, Baker P (2016) Natural hazards in australia: extreme bushfire. *Climatic Change* 139(1):85–99.

Shiryaev AN (1978) *Optimal stopping rules* (New York: Springer).

Siu TK (2016) A self-exciting threshold jump–diffusion model for option valuation. *Insurance: Mathematics and Economics* 69:168–193.

Solomon S (2007) *Climate change 2007 - the physical science basis: Working group I contribution to the fourth assessment report of the IPCC* (Cambridge University Press).

Stern N (2007) *The economics of climate change: the Stern review* (Cambridge University Press).

Tol RS, Yohe GW (2009) The Stern review: a deconstruction. *Energy Policy* 37(3):1032–1040.

Truong C, Trück S (2016) It's not now or never: Implications of investment timing and risk aversion on climate adaptation to extreme events. *European Journal of Operational Research* 253(3):856–868.

Truong C, Trück S, Mathew S (2018) Managing risks from climate impacted hazards–the value of investment flexibility under uncertainty. *European Journal of Operational Research* 269(1):132–145.

Waters D, Watt E, Marsalek J, Anderson B (2003) Adaptation of a storm drainage system to accommodate increased rainfall resulting from climate change. *Journal of Environmental Planning and Management* 46(5):755–770.

Weitzman ML (2009) On modeling and interpreting the economics of catastrophic climate change. *The Review of Economics and Statistics* 91(1):1–19.

West JJ, Small MJ, Dowlatabadi H (2001) Storms, investor decisions, and the economic impacts of sea level rise. *Climatic Change* 48(2-3):317–342.

Zhang X, Elliott RJ, Siu TK (2012) A Bayesian approach for optimal reinsurance and investment in a diffusion model. *Journal of Engineering Mathematics* 76(1):195–206.

Zhu TJ, Lund JR, Jenkins MW, Marques GF, Ritzema RS (2007) Climate change, urbanization, and optimal long-term floodplain protection. *Water Resources Research* 43(6):1–11.

Online Appendix

EC.1. The Esscher Transform

Recall that the stochastic benefit flow process $\{\pi_t\}$ follows a geometric Brownian motion so that the logarithm of benefit flow process follows a diffusion process with constant drift and volatility, which is a special case of a Lévy process. Consequently, the (classical) Esscher transform adopted in, for example, Gerber and Shiu (1993), which is applicable for Lévy processes, may be used here. However, with a view to incorporating time-varying or stochastic risk premiums here and to providing a general and rigorous approach to specifiy the density process for changing probability measures based on the Esscher transform, we use a generalized version of the Esscher transform for a semimartingale initially proposed by Bühlmann et al. (1996) and extended by Kallsen and Shiryaev (2002) and Siu (2016). The Esscher transform in this framework is based on the Doléan-Dade stochastic exponential and a Laplace cumulant process.

Recall from Section 2.3 that under the measure $\tilde{P}$, the dynamics of the stochastic intensity $\{\pi(t)\}$ are governed by the following geometric Brownian motion:

$$d\pi(t) = (\gamma + \mu_L)\pi(t)dt + \sigma\pi(t)d\tilde{B}(t).$$

We denote the Esscher parameter at time t by $\eta(t)$ and suppose that $\{\eta(t)\}$ is a real-valued predictable process with respect to the observed filtration $\{\mathcal{F}_t\}$. Also, for each t, let $Y(t) := \ln(\pi(t)/\pi(0))$. Then

$$dY(t) = \left(\gamma + \mu_L - \frac{1}{2}\sigma^2\right)dt + \sigma d\tilde{B}(t). \tag{EC.1}$$

Assume that the process $\{\eta(t)\}$ is such that the following stochastic integral exists:

$$(\eta \cdot Y)(t) := \int_0^t \eta(u)dY(u),$$

Then an $\{\mathcal{F}(t)\}$-special semimartingale $\{X^{\eta}(t)\}$ associated with the process of the Esscher parameters $\{\eta(t)\}$ is given by:

$$dX^{\eta}(t) := \left(\left(\gamma + \mu_L - \frac{1}{2}\sigma^2\right)\eta(t) + \frac{1}{2}\sigma^2\eta^2(t)\right)dt + \sigma\eta(t)d\tilde{B}(t). \tag{EC.2}$$

The predictable part $\{X_p^{\eta}(t)\}$ of the finite variation in $\{X^{\eta}(t)\}$ is:

$$X_p^{\eta}(t) = \int_0^t \left(\left(\gamma + \mu_L - \frac{1}{2}\sigma^2\right)\eta(u) + \frac{1}{2}\sigma^2\eta^2(u)\right)du.$$

As noted by Kallsen and Shiryaev (2002), $\{X_p^{\eta}(t)\}$ is the Laplace cumulant process of the stochastic integral process $\{(\eta \cdot Y)(t)\}$. Let $\{\mathcal{E}(X_p^{\eta})(t)\}$ be the stochastic exponential of $\{X_p^{\eta}(t)\}$. The density process of the generalized Esscher transform corresponding to the process $\{\eta(t)\}$, denoted as $\{Z^{\eta}(t)\}$, can then be defined as:

$$Z^{\eta}(t) := \frac{\exp((\eta \cdot Y)(t))}{\mathcal{E}(X_p^{\eta})(t)}. \tag{EC.3}$$

Note that the stochastic exponential $\{\mathcal{E}(X_p^{\eta})(t)\}$ acts as the normalisation constant, and therefore $Z^{\eta}(t)$ has a unit expected value. As noted in Siu (2016), since $\{X_p^{\eta})(t)\}$ is a finite variation process without martingale parts, we can write

$$\mathcal{E}(X_p^{\eta})(t) = \exp(X_p^{\eta}(t)). \tag{EC.4}$$

As a result:

$$Z^{\eta}(t) = \exp\left(\int_0^t \eta(u)\sigma d\tilde{B}(u) - \frac{1}{2}\int_0^t \eta^2(u)\sigma^2 du\right), \tag{EC.5}$$

which suggests that $Z^{\eta}(t)$ is a local-martingale with respect to $\{\mathcal{F}(t)\}$. Here we suppose that $\{\eta(t)\}$ satisfies the Novikov condition so that $\{Z^{\eta}(t)\}$ is an $\{\mathcal{F}(t)\}$-martingale.

EC.2. Proof of Lemma 2 on Immediate Stopping Value

The immediate stopping value $V(\phi_t, \pi_t)$ is obtained by setting the stopping time τ to t in (23),

$$V(\phi_t, \pi_t) = \int_t^{\infty} e^{-r(s-t)} E^{\eta} \left[(1+\phi_s)\pi_s | (\phi_t, \pi_t) \right] ds - (1+\phi_t) I. \tag{EC.6}$$

Since ϕ_t evolves according to Equation (20), its value at time $s > t$ is given by

$$\phi(s) = \phi(t) \exp[(\eta\omega)(s-t)] \hat{Z}_s \tag{EC.7}$$

where

$$\hat{Z}_s = \exp\left[-\frac{1}{2}\omega^2 (s-t) + \omega \int_t^s dB^{\eta}(u) \right] \tag{EC.8}$$

is a martingale with unit expected value, and can be used as a stochastic exponential. As a result,

$$E^{\eta}[\phi_s \pi_s | (\phi_t, \pi_t)] = \phi_t \exp[(\eta\omega)(s-t)] \pi_t \exp[(\gamma + \mu_H + \eta\sigma)(s-t)], \tag{EC.9}$$

where we use the fact that the stochastic exponential $\hat{Z}_s$ changes measure P^{η} to a new measure under which, π_t has a drift $\gamma + \mu_H + \eta\sigma$. The intrinsic value $V(\phi_t, \pi_t)$ then becomes

$$V(\phi_t, \pi_t) = \int_t^{\infty} e^{-r(s-t)} \left[\pi_t e^{(\gamma+\mu_L+\eta\sigma)(s-t)} + \phi_t \pi_t e^{(\gamma+\mu_H+\eta(\sigma+\omega))(s-t)} \right] ds - (1+\phi_t) I. \tag{EC.10}$$

which can be simplified to

$$V(\phi_t, \pi_t) = \frac{\pi_t}{r - \gamma - \mu_L - \eta\sigma} + \frac{\pi_t \phi_t}{r - \gamma - \mu_H - \eta(\sigma+\omega)} - (1+\phi_t) I. \blacksquare \tag{EC.11}$$

EC.3. Proof of Proposition 1 on Optimal Investment Boundary and Proposition 3 on Option Value

When $\gamma + \frac{\mu_H + \mu_L}{2} = \frac{1}{2}\sigma^2$, it follows from Equation (21) that:

$$\phi_s \pi_s^{-\omega/\sigma} = \phi_t \pi_t^{-\omega/\sigma}, \tag{EC.12}$$

which means that $\phi_s \pi_s^{-\omega/\sigma}$ does not change through time. Let $\theta = \phi_s \pi_s^{-\omega/\sigma}$, then:

$$G(\phi_t, \pi_t) = G(\theta \pi_t^{\omega/\sigma}, \pi_t) = J(\pi_t, \theta). \tag{EC.13}$$

In the continuation region, $J(\pi_t, \theta)$ must satify the second order partial differential equation:

$$\frac{1}{2}\sigma^2 \pi_t^2 J_{\pi\pi} + +(\mu_L + \eta_t \sigma)\pi_t J_\pi - rJ = 0. \tag{EC.14}$$

The general solution is given by:

$$J(\pi_t, \theta) = A(\theta)\pi_t^{\alpha_L} + B(\theta)\pi_t^{\delta}, \tag{EC.15}$$

where A and B are smooth functions to be determined and α_L and δ are the positive and negative roots of the quadratic equation:

$$\frac{1}{2}\sigma^2 \alpha(\alpha - 1) + (\gamma + \mu_L + \eta\sigma)\alpha - r = 0. \tag{EC.16}$$

The boundary condition $J(0, \theta) = 0$ implies $B = 0$. Hence,

$$G(\phi_t, \pi_t) = A(\phi_t \pi_t^{-\omega/\sigma})\pi_t^{\alpha_L}. \tag{EC.17}$$

At the investment boundary (ϕ^*, π^*), the value matching and smooth-pasting conditions must be satisfied:

$$G(\phi^*, \pi^*) = V(\phi^*, \pi^*) \tag{EC.18}$$

$$G_\phi(\phi^*, \pi^*) = V_\phi(\phi^*, \pi^*) \tag{EC.19}$$

$$G_\pi(\phi^*, \pi^*) = V_\pi(\phi^* \pi^*) \tag{EC.20}$$

which gives

$$A(\phi^*\pi^{*-\omega/\sigma})\pi^{*\alpha_L} = \frac{\pi^*}{r-\gamma-\mu_L-\eta\sigma} + \frac{\pi^*\phi^*}{r-\gamma-\mu_H-\eta(\sigma+\omega)} - (1+\phi^*)I \tag{EC.21}$$

$$\pi^{*-\omega/\sigma}A'\pi^{*\alpha_L} = \frac{\pi^*}{r-\gamma-\mu_H-\eta(\sigma+\omega)} - I \tag{EC.22}$$

$$-\frac{\omega}{\sigma}\phi^*\pi^{*-\omega/\sigma-1}A'\pi^{*\alpha_L} + \alpha_L A(\phi_t\pi^{*-\omega/\sigma})\pi^{*\alpha_L-1} = \frac{1}{r-\gamma-\mu_L-\eta\sigma} + \frac{\phi^*}{r-\gamma-\mu_H-\eta(\sigma+\omega)} \tag{EC.23}$$

Multiply (EC.23) by π^* and use (EC.21) and (EC.22) give:

$$\begin{aligned}
&-\frac{\omega}{\sigma}\phi^*\left[\frac{\pi^*}{r-\gamma-\mu_H-\eta(\sigma+\omega)} - I\right] + \\
&\alpha_L\left[\frac{\pi^*}{r-\gamma-\mu_L-\eta\sigma} + \frac{\pi^*\phi^*}{r-\gamma-\mu_H-\eta(\sigma+\omega)} - (1+\phi^*)I\right] \\
&= \frac{\pi^*}{r-\gamma-\mu_L-\eta\sigma} + \frac{\phi^*\pi^*}{r-\gamma-\mu_H-\eta(\sigma+\omega)}
\end{aligned} \tag{EC.24}$$

Rearrange terms:

$$(\alpha_L-1)\frac{\pi^*}{r-\gamma-\mu_L-\eta\sigma} + (\alpha_L-1-\omega/\sigma)\frac{\pi^*\phi^*}{r-\gamma-\mu_H-\eta(\sigma+\omega)} = \left[\alpha_L + \phi^*(\alpha_L-\omega/\sigma)\right]I$$

Let $\alpha_H = \alpha_L - \omega/\sigma$, and replace $\phi^* = P^*/(1-P^*)$ gives:

$$\pi^* = \frac{P^*\alpha_H + (1-P^*)\alpha_L}{P^*(\alpha_H-1)V_H + (1-P^*)(\alpha_L-1)V_L}I. \tag{EC.25}$$

where $V_L = \frac{1}{r-\gamma-\mu_L-\eta\sigma}$ and $V_H = \frac{1}{r-\gamma-\mu_H-\eta(\sigma+\omega)}$.

To prove Proposition 3, recall that $F(\phi_t,\pi_t) = \frac{1}{1+\phi_t}G(\phi_t,\pi_t)$, and $G(\phi_t,\pi_t) = A\pi_t^{\alpha_L}$. Using the value of A in (EC.21):

$$F(\phi_t,\pi_t) = \frac{1}{1+\phi_t}\frac{\pi^{*1-\alpha_L}\pi_t^{\alpha_L}}{r-\gamma-\mu_L-\eta\sigma} + \frac{1}{1+\phi_t}\frac{\phi^*\pi^{*1-\alpha_L}\pi_t^{\alpha_L}}{r-\gamma-\mu_H-\eta(\sigma+\omega)} - \frac{1+\phi^*}{1+\phi_t}\pi^{*-\alpha_L}\pi_t^{\alpha_L}I \tag{EC.26}$$

Since $\phi^*\pi^{*-\omega/\sigma} = \phi_t\pi_t^{-\omega/\sigma}$, and therefore $\phi^* = \phi_t\pi_t^{-\omega/\sigma}\pi^{*\omega/\sigma}$, it follows that:

$$F(\phi_t,\pi_t) = \frac{1}{1+\phi_t}\left(\frac{\pi_t}{\pi^*}\right)^{\alpha_L}\left(\frac{\pi^*}{r-\gamma-\mu_L-\eta\sigma} - I\right) + \frac{\phi_t}{1+\phi_t}\left(\frac{\pi_t}{\pi^*}\right)^{\alpha_H}\left(\frac{\pi^*}{r-\gamma-\mu_H-\eta(\sigma+\omega)} - I\right)$$

Replace $P_t = \frac{\phi_t}{1+\phi_t}$ and $1-P_t = \frac{1}{1+\phi_t}$ gives:

$$F(P_t,\pi_t) = P_t\left(\frac{\pi_t}{\pi^*}\right)^{\alpha_H}\left(\frac{\pi^*}{r-\gamma-\mu_H-\eta(\sigma+\omega)} - I\right) + (1-P_t)\left(\frac{\pi_t}{\pi^*}\right)^{\alpha_L}\left(\frac{\pi^*}{r-\gamma-\mu_L-\eta\sigma} - I\right) \blacksquare$$

EC.4. Proof of Proposition 2 on Decreasing Investment Boundary

The optimal investment threshold in (31) is:

$$\pi^* = \frac{P_t\alpha_H + (1-P_t)\alpha_L}{P_t(\alpha_H-1)V_H + (1-P_t)(\alpha_L-1)V_L} \times I \tag{EC.27}$$

where $V_H = \frac{1}{r-\gamma-\mu_H-\eta(\sigma+\omega)}$ and $V_L = \frac{1}{r-\gamma-\mu_L-\eta\sigma}$.

The derivative of π^* with respect to P_t is then:

$$\frac{\partial \pi^*}{\partial P_t} = \frac{(\alpha_H-\alpha_L)D - N[(\alpha_H-1)V_H - (\alpha_L-1)V_L]}{D^2} \times I, \tag{EC.28}$$

where N and D are the nominator, and denominator in (EC.27).

It follows that $\frac{\partial \pi^*}{\partial P_t}$ has the same sign as $S = (\alpha_H-\alpha_L)D - N[(\alpha_H-1)V_H - (\alpha_L-1)V_L]$. After multiplying the terms out, S is reduced to:

$$S = \alpha_H(\alpha_L-1)V_L - \alpha_L(\alpha_H-1)V_H. \tag{EC.29}$$

Using the expression of V_L, V_H, we can write S as:

$$S = \frac{[\alpha_H(\alpha_L-1)(r-\gamma-\mu_H-\eta(\sigma+\omega)) - \alpha_L(\alpha_H-1)(r-\gamma-\mu_L-\eta\sigma)]}{(r-\gamma-\mu_H-\eta(\sigma+\omega))(r-\gamma-\mu_L-\eta\sigma)}, \tag{EC.30}$$

and therefore, the sign of $\frac{\partial \pi^*}{\partial P_t}$ is the same as the sign of:

$$\hat{S} = \alpha_H(\alpha_L-1)(r-\gamma-\mu_H-\eta(\sigma+\omega)) - \alpha_L(\alpha_H-1)(r-\gamma-\mu_L-\eta\sigma). \tag{EC.31}$$

Since $\alpha_H = \alpha_L - \omega/\sigma$, we can write α_H as:

$$\alpha_H = \frac{1}{2} - (\gamma+\mu_H+\sigma\eta_t)/\sigma^2 + \sqrt{[(\gamma+\mu_L+\sigma\eta_t)/\sigma^2 - \frac{1}{2}]^2 + 2r/\sigma^2}$$

In addition, since $2\gamma+\mu_H+\mu_L = \sigma^2$, we can write:

$$[(\gamma+\mu_L+\sigma\eta_t)/\sigma^2 - \frac{1}{2}]^2 = [(\gamma+\mu_H-\sigma\eta_t)/\sigma^2 - \frac{1}{2}]^2 \tag{EC.32}$$

and therefore:

$$\alpha_H = -\frac{1}{2} - (\gamma+\mu_H+\sigma\eta_t)/\sigma^2 + \sqrt{[(\gamma+\mu_H-\sigma\eta_t)/\sigma^2 - \frac{1}{2}]^2 + 2r/\sigma^2}.$$

It follows that when $\eta = 0$, α_i where $i \in \{H, L\}$ satisfies Equation:

$$\frac{1}{2}\sigma^2\alpha_i(\alpha_i - 1) + (\gamma + \mu_i)\alpha_i - r = 0, \tag{EC.33}$$

which can be written as:

$$\alpha_i(r - \mu_i - \gamma) = (\alpha_i - 1)(\frac{1}{2}\sigma^2\alpha_i + r) \tag{EC.34}$$

Substitute (EC.34) into (EC.31) and use $\eta = 0$ gives:

$$\begin{aligned}\hat{S} =& (\alpha_L - 1)(\alpha_H - 1)(\frac{1}{2}\sigma^2\alpha_H + r)(\alpha_H - 1)(\alpha_L - 1)(\frac{1}{2}\sigma^2\alpha_L + r)\\ =& (\alpha_L - 1)(\alpha_H - 1)\frac{1}{2}\sigma^2(\alpha_H - \alpha_L)\\ =& -(\alpha_L - 1)(\alpha_H - 1)\frac{1}{2}\sigma^2(\omega/\sigma)\end{aligned} \tag{EC.35}$$

Since $\alpha_i > 1$ for $i \in \{L, H\}$ and $\omega/\sigma > 0$, it is clear that $\hat{S} < 0$, and $\frac{\partial \pi^*}{\partial P_t} < 0$. ∎

Note that the results by Décamps et al. (2005) and Klein (2009) are also easy to see. The investment threshold shown in Klein (2009) is:

$$\pi^* = I \times \frac{P_t\alpha_H + (1 - P_t)\alpha_L}{P_t(\alpha_H - 1) + (1 - P_t)(\alpha_L - 1)}, \tag{EC.36}$$

and so $\frac{\partial \pi^*}{\partial P_t}$ has the same sign as $\alpha_H(\alpha_L - 1) - \alpha_L(\alpha_H - 1)$. Since $\alpha_H = \alpha_L - \omega/\sigma$, we have $\alpha_H(\alpha_L - 1) = \alpha_L^2 - \alpha_L(1 + \omega/\sigma) + \omega/\sigma$; and also $\alpha_L(\alpha_H - 1) = \alpha_L^2 - \alpha_L(1 + \omega/\sigma)$. Since $\omega/\sigma > 0$ it follows that:

$$\alpha_H(\alpha_L - 1) > \alpha_L(\alpha_H - 1). \tag{EC.37}$$

Therefore, when the project is front-loaded as assumed by Décamps et al. (2005) and Klein (2009) $\frac{\partial \pi^*}{\partial P_t} > 0$.

EC.5. Proof of Lemma 3 on expected waiting time

For a process $dX_t = adt + \sigma dB_t$, where B_t is a Brownian motion, $X_0 = x > 0$, a stopping time $\tau_m = \min\{t \geq 0 : X_t = m\}$, and a scalar $u > 0$,

$$Ee^{-u\tau_m} = \exp\left[\frac{-a + \sqrt{a^2 + 2u\sigma^2}}{\sigma^2}(x - m)\right]. \tag{EC.38}$$

Then, taking the limit $\lim_{u\downarrow 0} \frac{\partial Ee^{-u\tau_m}}{\partial u}$ gives

$$E\tau_m = \frac{m - x}{a}. \tag{EC.39}$$

This result holds if $a > 0$ when $x < m$ or if $a \leq 0$ when $x > m$. The reason is if $a \leq 0$ when $x < m$, there is a positive probability that the process X_t wanders off to $-\infty$ and $E\tau_m$ is infinite.

For the proof of (EC.38), see e.g. Ryan and Lippman (2003).■

EC.6. Proof of Lemma 1 on the product of a martingale and an integral

Let $Y_s = \frac{1}{Z_s}$ and $X_s = \int_\tau^s e^{-r(u-t)}\pi_u du$ where $s \geq \tau \geq t$, then

$$H = \tilde{E}\left[Y_\infty X_\infty | (\phi_t, \pi_t)\right].$$

Applying Ito's product rule to $Y_s X_s$:

$$\begin{aligned} d(Y_s X_s) &= Y_s dX_s + X_s dY_s + d[Y,X]_s \\ &= \frac{1}{Z_s} e^{-r(s-t)}\pi_s ds + X_s dY_s. \end{aligned} \tag{EC.40}$$

Since $Z_s = \exp\left(-\int_0^s \theta_u d\bar{B}_u - \frac{1}{2}\int_0^s \theta_u^2 du\right)$ and $\tilde{B}_s = \bar{B}_s + \int_0^s \theta_u du$, Y_s is given by

$$Y_s = \frac{1}{Z_s} = \exp\left(\int_0^s \theta_u d\tilde{B}_u - \frac{1}{2}\int_0^s \theta_u^2 du\right),$$

and therefore $dY_s = Y_s \theta_s d\tilde{B}_s$. This implies that:

$$Y_\infty X_\infty = \int_\tau^\infty \frac{1}{Z_s} e^{-r(s-t)}\pi_s ds + \int_\tau^\infty X_s Y_s \theta_s d\tilde{B}_s, \tag{EC.41}$$

and as a result,

$$H = \tilde{E}\left[\int_\tau^\infty \frac{1}{Z_s} e^{-r(s-t)}\pi_s ds | (\phi_t, \pi_t)\right]. \blacksquare$$

EC.7. Binomial lattice method

A binomial lattice is constructed by first fixing a time horizon T and then dividing the time horizon into N small sub-intervals, each of which has a time length of $\Delta t = T/N$. At an arbitrary time step t of the binomial lattice, given the value Λ_t of the Poisson intensity, the value $\Lambda_{t+\Delta t}$ of the Poisson intensity at the next time step $t+\Delta t$ is either $\Lambda_t u$ with probability p or $\Lambda_t d$ with probability $1-p$, where $u = 1/d$. It is easy to see that the conditional mean and variance of $\Lambda_{t+\Delta t}$ given Λ_t are $p\Lambda_t u + (1-p)\Lambda_t d$, and $\Lambda_t^2[pu^2 + (1-p)d^2 - [pu + (1-p)d]^2]$, respectively. As shown by Cox et al. (1979), these conditional mean and variance are the same as those implied by the stochastic differential equation (12), which are $\Lambda_t e^{(\mu_L+\eta\sigma)\Delta t}$ and $\Lambda_t^2\sigma^2\Delta t$, when p, u, and d are set as follows:

$$u = e^{\sigma\sqrt{\Delta t}}, \qquad d = e^{-\sigma\sqrt{\Delta t}}, \qquad p = \frac{e^{(\mu_L+\eta\sigma)\Delta t} - d}{u - d}. \tag{EC.42}$$

For a given initial condition (ϕ_0, Λ_0), the value $G(\phi_0, \Lambda_0)$ is computed by backward induction, using Equation (25) and starting with the terminal condition $G(\phi_{T+1}, \Lambda_{T+1}) = 0$. The computational efficiency of the lattice method can be improved by applying the Richardson extrapolation as suggested by Boyle et al. (1989). The value of the option is calculated for 20, 40, 60, and 80 time steps per year and the obtained points are then fitted with a cubic polynomial. The value given by the polynomial curve at a high number of time steps then provides an accurate estimate of the option value. In empirical work, we use an investment time horizon of 100 years, since it seems that further increasing the investment time horizon may not have a material effect on the solution.

EC.8. Proof of Proposition 5 on the impact of uncertainty on optimal investment

Note that when $\gamma + \frac{\mu_H+\mu_L}{2} = \frac{1}{2}\sigma^2$ and $\eta = 0$, the optimal investment threshold under drift uncertainty is:

$$\pi^*(P_0) = \frac{P_0\alpha_H + (1-P_0)\alpha_L}{P_0(\alpha_H - 1)\frac{1}{r-\gamma-\mu_H} + (1-P_0)(\alpha_L - 1)\frac{1}{r-\gamma-\mu_L}} \times I, \tag{EC.43}$$

and the investment threshold for the case of known drift is:

$$\hat{\pi} = \frac{\hat{\alpha}}{(\hat{\alpha}-1)\frac{1}{r-\gamma-\hat{\mu}}} I.$$

Consider function $f = \frac{\alpha}{(\alpha-1)\frac{1}{r-\gamma-\mu}} I$. Note that α satisfies the equation:

$$\frac{1}{2}\sigma^2\alpha(\alpha-1) + (\gamma+\mu)\alpha - r = 0, \tag{EC.44}$$

which can be written as:

$$\alpha(r-\gamma-\mu) = (\alpha-1)(\frac{1}{2}\sigma^2\alpha + r). \tag{EC.45}$$

Using (EC.45) we can write f as

$$f = (\frac{1}{2}\sigma^2\alpha + r)I. \tag{EC.46}$$

Since $\alpha = \frac{1}{2} - (\gamma+\mu)/\sigma^2 + \sqrt{[(\gamma+\mu)/\sigma^2 - \frac{1}{2}]^2 + 2r/\sigma^2}$, the first and second derivative of α with respect to μ are:

$$\frac{\partial\alpha}{\partial\mu} = -\sigma^{-2} + \sigma^{-2}[(\frac{\gamma+\mu}{\sigma^2} - \frac{1}{2})^2 + 2r/\sigma^2]^{-1/2} \times (\frac{\gamma+\mu}{\sigma^2} - \frac{1}{2}) \tag{EC.47}$$

$$\frac{\partial^2\alpha}{\partial\mu^2} = \sigma^{-4}[(\frac{\gamma+\mu}{\sigma^2} - \frac{1}{2})^2 + 2r/\sigma^2]^{-1/2}[1 - (\frac{\gamma+\mu}{\sigma^2} - \frac{1}{2})^2[(\frac{\gamma+\mu}{\sigma^2} - \frac{1}{2})^2 + 2r/\sigma^2]^{-1}] > 0. \tag{EC.48}$$

It follows that f is convex in μ. Using the Jensen inequality, $\pi^* > \hat{\pi}$.■

EC.9. Proof of Proposition 4 on the Impact of Volatility on Optimal Investment

When $\eta = 0$, V_H and V_L do not depend on σ. The derivative of π^* with respect to σ is then:

$$\frac{\partial \pi^*}{\partial \sigma} = \frac{-P_t^2 V_H \times \frac{\partial \alpha_H}{\partial \sigma} - (1-P_t)^2 V_L \times \frac{\partial \alpha_L}{\partial \sigma}}{D^2} \times I, \tag{EC.49}$$

where D is the denominator in (31).

Since α_i, $i \in \{H, L\}$ satisfies Equation:

$$Q = \frac{1}{2}\sigma^2 \alpha_i(\alpha_i - 1) + \mu_i \alpha_i - r = 0, \tag{EC.50}$$

by total differentiation of (EC.50):

$$\frac{\partial Q}{\partial \alpha_i}\frac{\partial \alpha_i}{\partial \sigma} + \frac{\partial Q}{\partial \sigma} = 0, \tag{EC.51}$$

we then have:

$$\frac{\partial \alpha_i}{\partial \sigma} = -\frac{\partial Q/\partial \sigma}{\partial Q/\partial \alpha_i}. \tag{EC.52}$$

In addition, $\partial Q/\partial \sigma = \sigma \alpha_i(\alpha_i - 1) > 0$ since $\alpha_i > 1$. Also, Q is an upward pointing parabola with $Q(0) = -r < 0$ and therefore at $\alpha_i > 1$, we have $\partial Q/\partial \alpha_i > 0$. As a result, $\frac{\partial \alpha_i}{\partial \sigma} < 0$ and $\frac{\partial \pi^*}{\partial \sigma} > 0$. ■